[8] Y. Kuge, K. Minematsu, T. Yamaguchi, Y. Miyake, Nylon monofilament for intraluminal middle cerebral artery occlusion in rats, Stroke 26 (1995) 1655–1657 (discussion 1658).
[9] B. Lu, P.T. Pang, N.H. Woo, The yin and yang of neurotrophin action, Nat. Rev. Neurosci. 6 (2005) 603–614.
[10] A. Moraska, T. Deak, R.L. Spencer, D. Roth, M. Fleshner, Treadmill running produces both positive and negative physiological adaptations in Sprague–Dawley rats, Am. J. Physiol. Regul. Integr. Comp. Physiol. 279 (2000) R1321–R1329.
[11] S.J. Mowla, H.F. Farhadi, S. Pareek, J.K. Atwal, S.J. Morris, N.G. Seidah, R.A. Murphy, Biosynthesis and post-translational processing of the precursor to brain-derived neurotrophic factor, J. Biol. Chem. 276 (2001) 12660–12666.
[12] J. Nygren, M. Kokaia, T. Wieloch, Decreased expression of brain-derived neurotrophic factor in BDNF(+/−) mice is associated with enhanced recovery of motor performance and increased neuroblast number following experimental stroke, J. Neurosci. Res. 84 (2006) 626–631.
[13] A.L. Ohlsson, B.B. Johansson, Environment influences functional outcome of cerebral infarction in rats, Stroke 26 (1995) 644–649.
[14] M. Ploughman, S. Granter-Button, G. Chernenko, B.A. Tucker, K.M. Mearow, D. Corbett, Endurance exercise regimens induce differential effects on brain-derived neurotrophic factor, synapsin-I and insulin-like growth factor I after focal ischemia, Neuroscience 136 (2005) 991–1001.
[15] A. Risedal, B. Mattsson, P. Dahlqvist, C. Nordborg, T. Olsson, B.B. Johansson, Environmental influences on functional outcome after a cortical infarct in the rat, Brain Res. Bull. 58 (2002) 315–321.
[16] Y. Shono, C. Yokota, Y. Kuge, S. Kido, A. Harada, K. Kokame, H. Inoue, M. Hotta, K. Hirata, H. Saji, N. Tamaki, K. Minematsu, Gene expression associated with an enriched environment after transient focal ischemia, Brain Res. 1376 (2011) 60–65.
[17] H.K. Teng, K.K. Teng, R. Lee, S. Wright, S. Tevar, R.D. Almeida, P. Kermani, R. Torkin, Z.Y. Chen, F.S. Lee, R.T. Kraemer, A. Nykjaer, B.L. Hempstead, ProBDNF induces neuronal apoptosis via activation of a receptor complex of p75NTR and sortilin, J. Neurosci. 25 (2005) 5455–5463.
[18] K. Tureyen, N. Brooks, K. Bowen, J. Svaren, R. Vemuganti, Transcription factor early growth response-1 induction mediates inflammatory gene expression and brain damage following transient focal ischemia, J. Neurochem. 105 (2008) 1313–1324.
[19] L.R. Zhao, B. Mattsson, B.B. Johansson, Environmental influence on brain-derived neurotrophic factor messenger RNA expression after middle cerebral artery occlusion in spontaneously hypertensive rats, Neuroscience 97 (2000) 177–184.
[20] L.R. Zhao, A. Risedal, A. Wojcik, J. Hejzlar, B.B. Johansson, Z. Kokaia, Enriched environment influences brain-derived neurotrophic factor levels in rat forebrain after focal stroke, Neurosci. Lett. 305 (2001) 169–172.

Journal of Medicinal Chemistry

ARTICLE

pubs.acs.org/jmc

Novel ^{18}F-Labeled Benzofuran Derivatives with Improved Properties for Positron Emission Tomography (PET) Imaging of β-Amyloid Plaques in Alzheimer's Brains

Masahiro Ono,*[,†] Yan Cheng,[†] Hiroyuki Kimura,[†] Mengchao Cui,[†] Shinya Kagawa,[‡] Ryuichi Nishii,[‡] and Hideo Saji*[,†]

[†]Graduate School of Pharmaceutical Sciences, Kyoto University, 46-29 Yoshida Shimoadachi-cho, Sakyo-ku, Kyoto 606-8501, Japan

[‡]Shiga Medical Center Research Institute, 5-4-30, Moriyama, Moriyama City, Shiga 524-8524, Japan

Supporting Information

ABSTRACT: In vivo imaging of β-amyloid plaques in the brain may lead to the early diagnosis of Alzheimer's disease (AD) and monitoring of the progression and effectiveness of treatment. In the present study, we report on the development of two potential PET probes, [^{18}F]FPYBF-2 ([^{18}F]**10**) and [^{18}F]FPHBF-2 ([^{18}F]**21**), for imaging of β-amyloid plaques in AD brain. In experiments in vitro, **10** and **21** displayed high affinity for Aβ(1−42) aggregates (K_i = 2.41 and 3.85 nM, respectively). In biodistribution experiments using normal mice, they displayed high uptake in the brain (7.38 and 8.18% ID/g at 2 min postinjection, respectively), and the radioactivity washed out from the brain rapidly (3.15 and 3.87% ID/g at 60 min postinjection, respectively), which is highly desirable for β-amyloid imaging agents. In vivo, they clearly labeled β-amyloid plaques in Tg2576 mice. Furthermore, the specific labeling of β-amyloid plaques by **10** and **21** was observed in autoradiographs of sections of autopsied AD brain. These new fluorinated benzofuran derivatives are promising PET probes for imaging cerebral β-amyloid plaques.

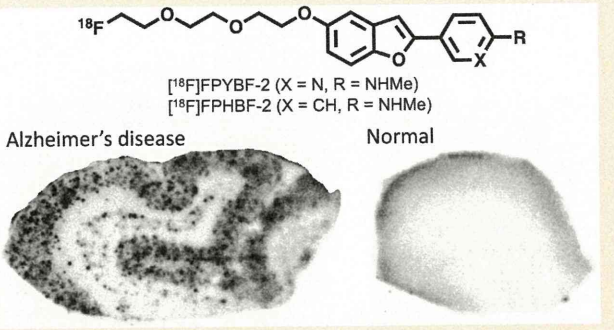

INTRODUCTION

Alzheimer's disease (AD), the most common senile dementia, is characterized by β-amyloid (Aβ) plaques, vascular amyloid, neurofibrillary tangles, and progressive neurodegeneration. The formation of Aβ plaques, composed of Aβ peptides, in the brain is generally accepted as the initial neurodegenerative event in AD.[1,2] The in vivo detection of Aβ plaques in AD brains by positron emission tomography (PET) should be useful for early diagnosis and the discovery of effective therapeutic agents for AD.[3−5]

Initial studies with PET suggested that [^{11}C]4-*N*-methylamino-4′-hydroxystilbene (SB-13),[6,7] [^{11}C]2-(4′-(methylamino phenyl)-6-hydroxybenzothiazole (PIB),[8,9] [^{11}C]2-(2-[2-dimethylaminothiazol-5-yl]ethenyl)-6-(2-[fluoro]ethoxy)benzoxazole (BF-227),[10] and [^{11}C]-2-[6-(methylamino)pyridin-3-yl]-1,3-benzothiazol-6-ol (AZD2184),[11,12] differed in their uptake and retention in the brain between AD patients and controls (Figure 1). Among them, PIB is the best characterized PET imaging agent for Aβ plaques in the brain. In the past few years, successful imaging with PIB in thousands of AD patients has been reported. The utility of PIB to image Aβ plaques in the brain has provided considerable impetus for further refinement of this technique. However, the practical challenges of using PIB labeled with ^{11}C ($t_{1/2}$ = 20 min) on a routine basis have limited its potential as a diagnostic tool. Since additional tracers labeled with ^{18}F with longer half-life ($t_{1/2}$ = 110 min) may be more useful as PET imaging agents for detection and quantification of Aβ plaques, recent efforts have focused on the development of comparable agents labeled with ^{18}F. Previous studies with [^{18}F]2-(1-(2-(*N*-(2-fluoroethyl)-*N*-methylamino)naphthalene-6-yl)ethylidene)malononitrile (FDDNP)[13,14] showed differential uptake and retention in the brain of AD patients for the first time. PET imaging studies in humans suggest that FDDNP shows a higher retention in regions of the brain suspected of having neurofibrillary tangles and Aβ plaques, indicating that it is not for selectively measuring Aβ plaques in AD brains. More recently, a PIB analogue, 2-(3-[^{18}F]fluoro-4-methyaminophenyl)benzothiazol-6-ol (GE-067, flutemetamol),[15−17] a stilbene derivative, (*E*)-4-(*N*-methylamino)-4′-(2-(2-(2-[^{18}F]fluoroethoxy)ethoxy)ethoxy)stilbene (BAY94-9172, florbetaben) ,[18−20] and a styrylpyridine derivative, (*E*)-4-(2-(6-(2-(2-(2-([^{18}F]fluoroethoxy)ethoxy)ethoxy)pyridyn-3-ylvinyl)-*N*-methylbenzenamine (AV-45, florbetapir),[21−27] and have been shown to

Received: January 20, 2011
Published: March 23, 2011

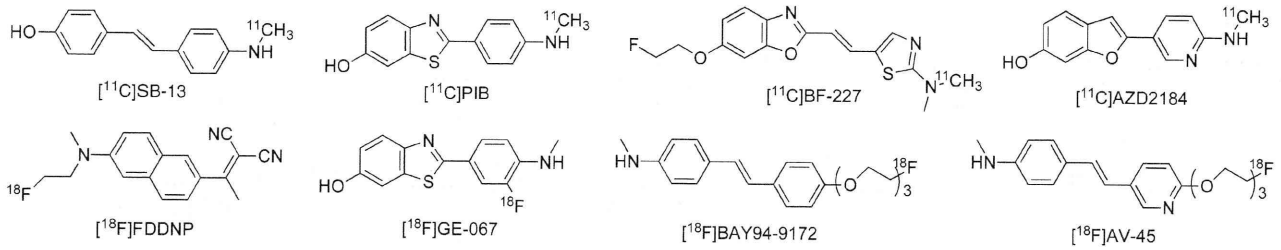

Figure 1. Chemical structures of PET imaging agents targeting β-amyloid plaques in AD patients.

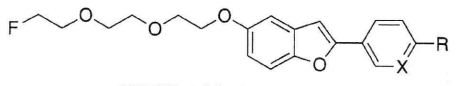

FPYBF-1 (X = N, R = NMe_2)
FPHBF-1 (X = CH, R = NMe_2)
FPYBF-2 (**10**) (X = N, R = NHMe)
FPHBF-2 (**21**) (X = CH, R = NHMe)

Figure 2. Chemical structure of ^{18}F-labeled benzofuran derivatives reported in the present study.

be useful for the imaging of Aβ plaques in living brain tissue in phase II or III clinical trials (Figure 1).

In the search for PET imaging agents with improved properties, we have recently reported a series of fluorinated benzofuran derivatives as potential ^{18}F-labeled tracers for the imaging of Aβ plaques by PET. First, on the basis of our previous research regarding radioiodinated and ^{11}C-labeled benzofuran derivatives,[28,29] we developed 4-(5-(2-(2-(2-fluoroethoxy)-ethoxy)ethoxy)benzofuran-2-yl)-*N*,*N*-dimethylbenzenamine (FPHBF-1, Figure 2) with a fluoropolyethylene glycol side chain and a dimethyaminophenyl group.[30] Although the penetration of brain tissues by this tracer was encouraging, the slow washout of this probe from the normal mouse brain made it unsuitable for imaging in vivo. Therefore, a critical need to fine-tune the kinetics of the uptake and washout of benzofuran derivatives existed. Previous results regarding uptake into and clearance from the brain point to high lipophilicity as one of the reasons for a slow washout from the brain.[8,29,31,32]

To further improve the pharmacokinetics of the radioactivity in the brain, we planned to develop a novel fluorinated pyridylbenzofuran derivative with less lipophilicity by displacing the phenyl group in phenylbenzofuran with a pyridyl group. Then we designed and synthesized 5-(5-(2-(2-(2-fluoroethoxy)ethoxy)ethoxy)benzofuran-2-yl)-*N*,*N*-dimethylpyridin-2-amine (FPYBF-1, Figure 2) with a fluoropolyethylene glycol side chain and a dimethylaminopyridyl group.[33] This tracer displayed faster clearance from the normal mouse brain than FPHBF-1, without a decrease in uptake and reduction in affinity for Aβ plaques. These results suggested that the pharmacokinetics were improved by reducing the lipophilicity of the benzofuran derivative. While ^{18}F-labeled AV-19 ((*E*)-2-(2-(2-(2-fluoroethoxy)ethoxy)ethoxy)-5-(4-dimethylaminostyryl)pyridine) showed promising results in animal studies, its uptake in humans was lower than expected possibly because of a rapid metabolism of its dimethylamino group.[27] However, monomethylation of AV-19 led to the formation of AV-45, which exhibited excellent uptake and washout in the brain in humans.[22,27] Furthermore, all PET imaging probes in phase III clinical trials (AV-45, BAY94-9172, and GE067, Figure 1) have a monomethylamino group that is stable in vivo and reduces the lipophilicity of the compounds compared with a dimethylamino group.

In the present study, we designed and synthesized novel fluorinated pyridylbenzofuran and phenylbenzofuran derivatives (FPYBF-2 and FPHBF-2, Figure 2) with a fluoropolyethylene glycol side chain and a monomethylamino group. We here report the synthesis and biological evaluation of two new ^{18}F benzofuran derivatives with a monomethylamino group in comparison with the corresponding benzofuran derivatives with a dimethylamino group.

RESULTS AND DISCUSSION

The synthesis of FPYBF-2 (**10**) and FPHBF-2 (**21**) is outlined in Schemes 1 and 2, respectively. The key step in the formation of the fluorinated pyridylbenzofuran backbone is accomplished by Suzuki coupling between 5-methoxybenzofuran-2-boronic acid and 2-amino-5-iodopyridine.[34] Suzuki coupling afforded the desired compound **1** in a yield of 52%. The key step in the formation of the phenylbenzofuran backbone was readily achieved by reacting 2-hydroxy-5-methoxybenzaldehyde with 4-nitrobenzyl bromide to produce **11** in a yield of 64%. The amino derivative **12** was prepared from **11** by reduction with $SnCl_2$ in a yield of 49%. Conversion of **1** and **12** to the monomethylamino derivatives **2** and **13** was achieved by the monomethylation of the amino group by using a method[29] previously reported in yields of 92% and 95%, respectively. A methoxy group of **2** and **13** was converted to a hydroxyl group using BBr_3/CH_2Cl_2, which afforded **3** and **14** in yields of 99 and 99%, respectively. To prepare compounds with three ethoxy groups as the polyethylene glycol linkage, 2-[2-(2-chloroethoxy)ethoxy]ethanol was coupled with the OH group of **3** and **14** to obtain **4** and **15**. The free OH groups of **4** and **15** were subsequently protected with *tert*-butyldimethylsilyl chloride (TBDMSCl) to give **5** and **16**. Compounds **6** and **17** were obtained by protecting the methylamino groups of **5** and **16**. After removal of the TBS-protected groups of **5** and **16** with tetrabutylammonium fluoride (TBAF) in tetrahydrofuran (THF), the free OH groups of **7** and **18** were converted into mesylates by reacting with MsCl in the presence of triethylamine to give **8** and **19**. The fluorinated benzofuran derivatives **10** and **21** were successfully obtained by refluxing **8** and **19** in anhydrous TBAF/THF followed by stirring with TFA to remove the butyloxycarbonyl (BOC) protected group.

To prepare the desired ^{18}F-labeled benzofuran derivatives, the *N*-BOC-protected mesylates **8** and **19** were employed as the precursors (Scheme 3). Each of the mesylates was reacted with [^{18}F]fluoride/potassium carbonate and Kryptofix 222 in acetonitrile. The mixture was then treated with aqueous HCl to remove the *N*-BOC-protected group. After purification of the crude product by HPLC, the ^{18}F-labeled **10** ([^{18}F]FPYBF-2) and **21** ([^{18}F]FPHBF-2) were prepared with an average radiochemical

Scheme 1[a]

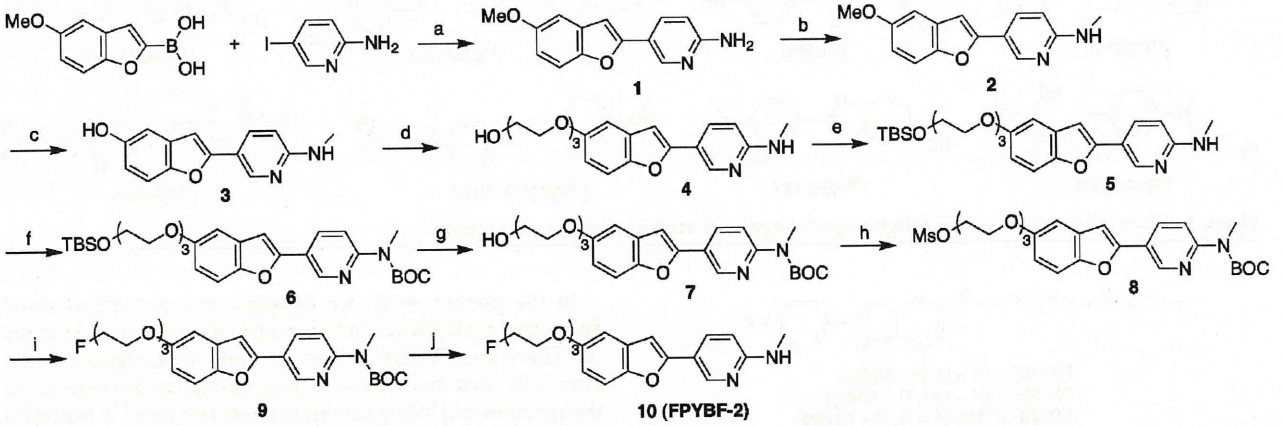

[a] Reagents: (a) $(Ph_3P)_4Pd$, Na_2CO_3(aq)/dioxane; (b) (1) NaOMe, MeOH, $(CH_2O)_n$; (2) $NaBH_4$; (c) BBr_3, CH_2Cl_2; (d) 2-[2-(2-chloroethoxy)ethoxy]ethanol, K_2CO_3, DMF; (e) TBDMSCl, imidazole, CH_2Cl_2; (f) $(BOC)_2O$, THF; (g) TBAF, THF; (h) MsCl, Et_3N, CH_2Cl_2; (i) TBAF, THF; (j) TFA, CH_2Cl_2.

Scheme 2[a]

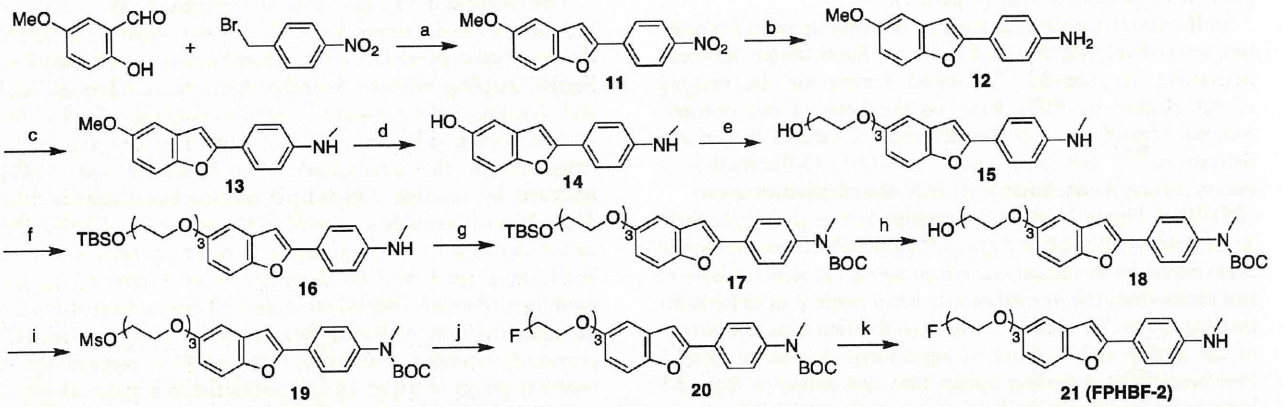

[a] Reagents: (a) K_2CO_3, DMF; (b) $SnCl_2$, EtOH; (c) NaOMe, $(CH_2O)_n$, MeOH; (d) BBr_3, CH_2Cl_2; (e) 2-[2-(2-chloroethoxy)ethoxy]ethanol, K_2CO_3, DMF; (f) TBDMSCl, imidazole, CH_2Cl_2; (g) $(BOC)_2O$, THF; (h) TBAF, THF; (i) MsCl, Et_3N, CH_2Cl_2; (j) TBAF, THF; (k) TFA, CH_2Cl_2.

Scheme 3[a]

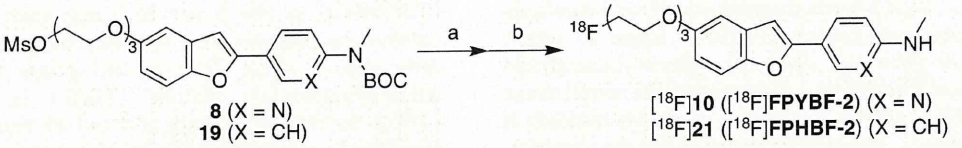

[a] Reagents and conditions: (a) Kryptofix 222/K_2CO_3, $^{18}F^-$, MeCN, 120 °C, 5 min; (b) 10%HCl (aq), 120 °C, 5 min.

yield of 52% and radiochemical purity of >99% and a specific activity of 242 GBq/μmol. The identity of [^{18}F]**10** and [^{18}F]**21** was verified by a comparison of the retention time with that of the nonradioactive compound (see Supporting Information).

Experiments in vitro to evaluate the affinity of the fluorinated benzofuran derivatives for Aβ aggregates were carried out in solutions with [^{125}I]2-(4′-dimethylaminophenyl)-6-iodoimidazo[1,2-*a*]pyridine ([^{125}I]IMPY) as the ligand according to conventional methods.[35,36] Compounds **10** and **21** inhibited the binding of [^{125}I]IMPY with a K_i of 2.41 and 3.85 nM, respectively, indicating that they have excellent affinity for Aβ(1−42) aggregates (Table 1). The *N*-monomethylated derivatives (**10** and **21**) exhibited slightly less affinity (K_i = 2.41 and 3.85 nM, respectively) than the N,N-dimethylated derivatives (FPYBF-1 and FPHBF-1) (0.95 and 2.00 nM, respectively). In addition, **10** and **21** showed higher binding affinity than PIB and IMPY, well-known Aβ imaging probes (K_i = 9.00 and 10.5 nM, respectively), in the same assay. The result suggests that removing the methyl group from a dimethylamino group of FPYBF-1 and FPHBF-1 reduces the affinity for Aβ aggregates. It also indicates that the electronegativity of the nitrogen

dx.doi.org/10.1021/jm200057u |*J. Med. Chem.* 2011, 54, 2971–2979

Table 1. Inhibition Constants of Benzofuran Derivatives on Binding to Aβ42 Aggregates

compd	K_i (nM)[a]	ClogP[b]
10	2.41 ± 0.11	2.32
21	3.85 ± 0.22	2.94
FPYBF-1	0.95 ± 0.21	3.11
FPHBF-1	2.00 ± 0.50	3.73
PIB	9.00 ± 1.31	3.28
IMPY	10.50 ± 1.05	3.79

[a] Values are the mean ± standard error of the mean for three independent experiments. [b] The calculated logarithms of water−octanol partition coefficients (ClogP) were obtained using ChemDraw Ultra 10.0 software (CambridgeSoft, Cambridge, MA).[46]

Table 2. Biodistribution of Radioactivity after Intravenous Administration of ^{18}F-Labeled Benzofuran Derivatives in Mice[a]

	time after injection (min)			
tissue	2	10	30	60
		[^{18}F]**10**		
blood	4.96 (0.38)	3.02 (0.12)	2.66 (0.34)	2.42 (0.13)
brain	7.38 (0.84)	4.86 (0.41)	4.03 (0.61)	3.15 (0.10)
bone	2.65 (0.35)	1.63 (0.13)	1.79 (0.17)	1.72 (0.27)
liver	16.8 (2.20)	17.5 (1.81)	19.2 (2.64)	8.71 (0.99)
kidney	11.9 (0.93)	6.22 (0.66)	7.83 (1.18)	3.70 (1.79)
intestine	4.24 (0.51)	8.39 (2.04)	24.1 (5.76)	30.9 (8.00)
spleen	2.91 (0.42)	2.15 (0.14)	3.14 (0.61)	2.24 (0.35)
lung	5.68 (0.33)	3.12 (0.21)	4.34 (0.77)	2.88 (0.27)
pancreas	5.14 (0.48)	2.68 (0.29)	4.91 (2.21)	2.55 (0.21)
heart	5.19 (0.39)	2.51 (0.28)	3.59 (0.48)	2.60 (0.23)
stomach[b]	3.73 (0.81)	7.55 (2.09)	18.8 (5.69)	22.5 (2.56)
		[^{18}F]**21**		
blood	4.10 (0.56)	4.17 (0.32)	5.33 (0.33)	7.33 (1.01)
brain	8.18 (0.59)	6.43 (0.66)	4.26 (0.42)	3.87 (0.42)
bone	1.57 (0.62)	1.98 (0.16)	2.07 (0.16)	3.30 (0.25)
		[^{18}F]FPYBF-1		
blood	2.83 (0.89)	2.13 (0.49)	1.76 (0.09)	1.98 (0.35)
brain	5.16 (0.30)	3.75 (0.64)	2.78 (0.22)	2.44 (0.36)
bone	1.61 (0.33)	1.33 (0.28)	1.11 (0.13)	1.42 (0.24)
		[^{18}F]FPYBF-1		
blood	1.64 (0.07)	2.48 (0.18)	2.68 (0.26)	3.41 (0.56)
brain	2.88 (0.46)	5.66 (0.31)	3.14 (0.26)	2.80 (0.06)
bone	1.19 (0.18)	1.76 (0.13)	3.63 (1.11)	2.74 (0.59)

[a] Expressed as % injected dose per gram. Each value represents the mean (SD) for five animals at each interval. [b] Expressed as % injected dose per organ.

atom of the aminophenyl group plays an important role in determining binding affinity. A similar change in affinity for Aβ aggregates after *N*-methyl groups were added has been observed for stilbene,[37] styrylpyridine,[38] flavone,[31] chalcone,[39] and aurone[40] derivatives containing a *p*-aminophenyl group.

To evaluate the uptake of [^{18}F]**10** and [^{18}F]**21** in the brain, a biodistribution experiment was performed in normal mice (Table 2).

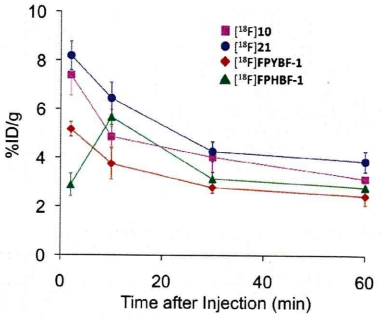

Figure 3. Comparison of brain uptake of four ^{18}F-labeled benzofuran derivatives in normal mice.

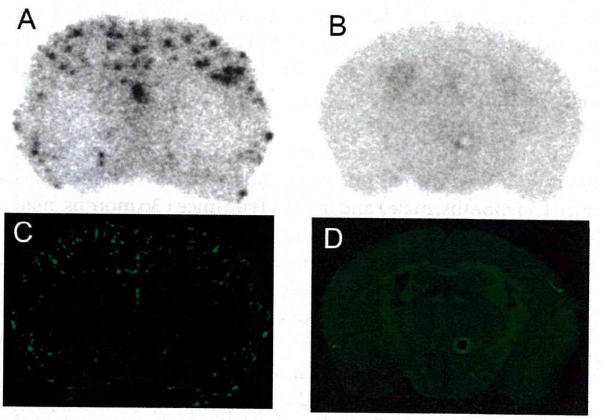

Figure 4. Ex vivo plaque labeling in brain sections from a Tg2576 mouse (A) and a wild-type mouse (B) with [^{18}F]**10**. The same sections were also stained with thioflavin-S (C, D).

[^{18}F]**10** and [^{18}F]**21** displayed high uptake (7.38 and 8.18% ID/g) at 2 min postinjection; these values were comparable to those reported for BAY94-9172 and AV-45, which are under phase III clinical trials. The uptake of [^{18}F]**10** and [^{18}F]**21** was higher than that of [^{18}F]FPYBF-1 and [^{18}F]FPHBF-1 with a dimethylamino group. The radioactivity in the brain after the injection of [^{18}F]**10** and [^{18}F]**21** cleared with time (3.15 and 3.87% ID/g at 60 min postinjection). Since there are no Aβ plaques in the brain of normal mice, a high initial uptake and rapid washout in normal mouse brain are highly desirable properties for Aβ plaque-targeting imaging agents. To directly compare the uptake and washout of four ligands tested in this study, a combined plot is presented in Figure 3. The $\text{brain}_{2\text{min}}/\text{brain}_{60\text{min}}$ ratio as an index to compare the washout rate is used for determining the radioactivity pharmacokinetics in vivo.[40] The $\text{brain}_{2\text{min}}/\text{brain}_{60\text{min}}$ ratio of [^{18}F]**10**, [^{18}F]**21**, [^{18}F]FPYBF-1, and [^{18}F]FPHBF-1 was 2.34, 2.11, 2.11, and 1.02, respectively, indicating that [^{18}F]**10** provided the best profile of radioactivity in the brain among the four ligands. Although the $\text{brain}_{2\text{min}}/\text{brain}_{60\text{min}}$ ratio of [^{18}F]**10** (2.34) was lower than that of [^{18}F]BAY94-9172 (4.8)[18] or [^{18}F]AV-45 (3.8),[21] it was improved compared to values for [^{18}F]FPYBF-1 (2.11) reported previously.[30] The favorable in vivo pharmacokinetics of [^{18}F]**10** were achieved by changing the dimethylaminophenyl group in [^{18}F]FPYBF-1 to a monomethylaminophenyl group. Although lipophilicity is just one of the factors affecting the uptake of a compound into the brain, previous results suggest the lipophilicity of Aβ imaging agents to play an important role in uptake and washout. The results observed for [^{18}F]**10** and

dx.doi.org/10.1021/jm200057u |J. Med. Chem. 2011, 54, 2971–2979

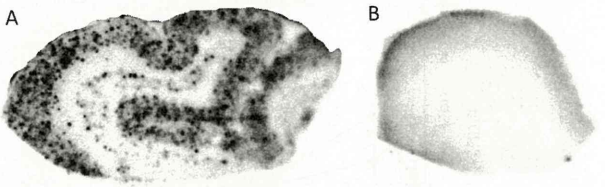

Figure 5. In vitro autoradiograms of sections of AD brain labeled with [^{18}F]**10**. Intensive labeling of β-amyloid plaques in brain tissue from AD patients is shown (A). The control subject exhibits no labeling by this tracer (B).

[^{18}F]**21** suggest that the introduction of further hydrophilic groups into the pyridylbenzofuran and phenylbenzofuran scaffold may lead to the development of more useful pyridylbenzofuran and phenylbenzofuran derivatives. No marked uptake of [^{18}F]**10** and [^{18}F]**21** in the bone was observed (1.72 and 3.30% ID/g, respectively), suggesting little defluorination in vivo, and so interference with the imaging is expected to be relatively minor.

To further characterize the potential of these probes in living brain tissue, we carried out autoradiography ex vivo in Tg2576 mice (36 months, male) and in wild-type mice (36 months, male) as age-matched controls (Figure 4). Tg2576 transgenic mice show marked Aβ deposition in the brain by 11−13 months of age[41] and have been frequently used to evaluate the specific binding of Aβ plaques in experiments in vitro and in vivo.[39,42,43] The autoradiography using [^{18}F]**10** showed distinctive labeling of Aβ plaques in the Tg2576 mouse brain (Figure 4A), while wild-type mouse brain showed no such labeling (Figure 4B). Aβ plaques were confirmed to be present by costaining the sections with thioflavin-S, a dye commonly used to stain Aβ plaques (Figure 4C). When we carried out ex vivo autoradiography in Tg2576 using [^{18}F]**21**, we obtained almost the same results as with [^{18}F]**10** (data not shown). The results suggest that these probes penetrated the blood−brain barrier and selectively labeled the Aβ plaques in the brain, as reflected by the biodistribution experiments and the in vitro binding assays.

Furthermore, we also investigated the effectiveness for neuropathological staining of Aβ plaques in human AD brain sections (Figure 5). A previous report suggested the configuration/folding of Aβ plaques in Tg2576 mice to be different from the tertiary/quaternary structure of Aβ plaques in AD brains.[44] Therefore, it is important to evaluate the affinity for Aβ plaques in human AD brains. [^{18}F]**10** clearly stained many Aβ plaques in AD brains. In contrast, no apparent staining was observed in normal adult brain sections. The labeling pattern was consistent with that observed by immunohistochemical labeling with an antibody specific to Aβ. The same results were observed in in vitro autoradiography using [^{18}F]**21** (data not shown). These results indicate that [^{18}F]**10** may be applicable for in vivo imaging of Aβ plaques in AD brains and deserves further investigation as a potential probe for the diagnosis of AD.

In conclusion, on the basis of previous results, we designed and synthesized two novel fluorinated pyridylbenzofuran and phenylbenzofuran ligands **10** and **21** for the imaging of Aβ plaques in the brain. These ligands showed high affinity for Aβ aggregates in vitro and for Aβ plaques in sections of autopsied AD brain. In biodistribution experiments using normal mice, they displayed good uptake into and fast washout from the brain, especially [^{18}F]**10**. In addition, ex vivo autoradiograms of brain sections from Tg2576 mice after the injection of [^{18}F]**10** showed selective binding of Aβ plaques with little nonspecific binding. The results suggest that [^{18}F]**10** should be further investigated as a potentially useful PET imaging agent for cerebral Aβ plaques. [^{18}F]**10** is currently in preparation for clinical trials.

EXPERIMENTAL SECTION

General Remarks. All chemicals used in syntheses were commercial products used without further purification. ^{1}H NMR spectra were obtained at 400 MHz on JEOL JNM-AL400 NMR spectrometers at room temperature with TMS as an internal standard. Chemical shifts are reported as δ values relative to the internal TMS. Coupling constants are reported in hertz. Multiplicity is defined by s (singlet), d (doublet), t (triplet), and m (multiplet). Mass spectra were acquired with a Shimadzu GC-MS-QP2010 Plus (ESI). HPLC was performed with a Shimadzu system (a LC-10AT pump with a SPD-10A UV detector, λ = 254 nm) with a Cosmosil C_{18} column (Nakalai Tesque, 5C_{18}-AR-II, 4.6 mm × 150 mm) using acetonitrile/water (60:40) as the mobile phase at a flow rate of 1.0 mL/min. Fluorescent observation was performed by microscope (Nikon Eclipse 80i) with a BV-2A filter set (excitation, 400−440 nm; diachronic mirror, 455 nm; long pass filter, 470 nm). All key compounds were proven to show ≥95% purity by HPLC.

Chemistry. 5-(5-Methoxy-2-benzofuranyl)-2-pyridinamine (1). A solution of 5-methoxybenzofuran-2-boronic acid (576 mg, 3.0 mmol), 2-amino-5-iodopyridine (660 mg, 3.0 mmol), and $(Ph_3)_4Pd$ (366 mg, 0.3 mmol) in 2 M Na_2CO_3/dioxane (150 mL, 1:1) was stirred under reflux overnight. After the mixture had cooled to room temperature, 1 M NaOH (20 mL) was added and extraction with ethyl acetate was carried out. The organic phase was dried over Na_2SO_4 and filtered. The filtrate was concentrated and the residue was purified by silica gel chromatography (hexane/ethyl acetate = 1:1) to give 374 mg of **1** (52.1%). ^{1}H NMR (400 MHz, $CDCl_3$): δ 3.85 (s, 3H), 4.67 (s, 2H), 6.59 (d, 1H, J = 8.8 Hz), 6.76 (s, 1H), 6.82 (dd, 1H, J_1= 8.8 Hz, J_2= 2.4 Hz), 7.07 (d, 1H, J = 2.4 Hz), 7.36 (d, 1H, J = 8.8 Hz), 7.86 (dd, 1H, J_1= 8.8 Hz, J_2= 2.4 Hz), 8.67 (d, 1H, J = 2.4 Hz). MS: m/z 241 (M^+ + H).

5-(5-Methoxy-2-benzofuranyl)-*N*-methyl-2-pyridinamine (2). Sodium methoxide (275 mg, 5.0 mmol) was added to **1** (240 mg, 1.0 mmol) in methanol (15 mL) followed by paraformaldehyde (101 mg, 4.0 mmol). The solution was heated to reflux for 2 h and cooled to 0 °C with an ice bath. Sodium borohydride (128 mg, 4.0 mmol) was added. The reaction mixture was brought to reflux again for 1 h and poured onto crushed ice. After a standard workup with ethyl acetate, the residue was purified by silica gel chromatography (hexane/ethyl acetate = 1:1) to give 234 mg of **2** (92.1%). ^{1}H NMR (400 MHz, $CDCl_3$): δ 2.98 (d, 3H, J = 5.2 Hz), 3.84 (s, 3H), 4.78 (s, 1H), 6.47 (d, 1H, J = 8.8 Hz), 6.76 (s, 1H), 6.84 (dd, 1H, J_1 = 8.8 Hz, J_2 = 4.4 Hz), 7.00 (d, 1H, J = 2.4 Hz), 7.36 (d, 1H, J = 8.4 Hz), 7.87 (dd, 1H, J_1 = 8.8 Hz, J_2 = 2.4 Hz), 8.59 (d, 1H, J = 2.8 Hz). MS: m/z 255 (M^+ + H).

2-(6-Methylamino-3-pyridinyl)-5-benzofuranol (3). BBr_3 (4.8 mL, 1 M solution in CH_2Cl_2) was added to a solution of **2** (234 mg, 0.92 mmol) in CH_2Cl_2 (20 mL) dropwise in an ice bath. The mixture was allowed to warm to room temperature and stirred for 1 h. Water (20 mL) was added while the reaction mixture was cooled in an ice bath. The mixture was extracted with ethyl acetate, and the organic phase was dried over Na_2SO_4 and filtered. The filtrate was concentrated, and the residue was purified by silica gel chromatography (hexane/ethyl acetate = 1:1) to give 218 mg of **3** (99.0%). ^{1}H NMR (400 MHz, $CDCl_3$): δ 2.98 (d, 3H, J = 5.2 Hz), 4.78 (s, 1H), 6.47 (d, 1H, J = 8.8 Hz), 6.76 (s, 1H), 6.84 (dd, 1H, J_1 = 8.8 Hz, J_2 = 4.4 Hz), 7.00 (d, 1H, J = 2.4 Hz), 7.36 (d, 1H, J = 8.4 Hz), 7.87 (dd, 1H, J_1 = 8.8 Hz, J_2 = 2.4 Hz), 8.59 (d, 1H, J = 2.8 Hz). MS: m/z 241 (M^+ + H).

2-(2-(2-(2-(6-(Methylamino)-3-pyridinyl)-5-benzofuranyloxy)ethoxy)ethoxy)ethanol (4). To a solution of **3** (197 mg, 0.82

mmol) and 2-[2-(2-chloroethoxy)ethoxy]ethanol (180 μL, 1.20 mmol) in DMF (5 mL) was added anhydrous K_2CO_3 (414 mg, 3.0 mmol). The reaction mixture was stirred for 18 h at 100 °C and then poured into water and extracted with chloroform. The organic layers were combined and dried over Na_2SO_4. Evaporation of the solvent afforded a residue, which was purified by silica gel chromatography (hexane/ethyl acetate = 1:6) to give 224 mg of **4** (60.3%). ^{1}H NMR (400 MHz, $CDCl_3$): δ 2.98 (d, 3H, J = 5.2 Hz), 3.62 (d, 2H, J = 4.4 Hz), 3.70−3.74 (m, 6H), 3.84 (s, 2H), 4.11 (s, 2H), 5.18 (s, 1H), 6.47 (d, 1H, J = 8.8 Hz), 6.76 (s, 1H), 6.84 (dd, 1H, J_1 = 8.8 Hz, J_2 = 4.4 Hz), 7.00 (d, 1H, J = 2.4 Hz), 7.36 (d, 1H, J = 8.4 Hz), 7.87 (dd, 1H, J_1 = 8.8 Hz, J_2 = 2.4 Hz), 8.59 (d, 1H, J = 2.8 Hz). MS: m/z 373 ($M^+ + H$).

5-(5-(2-(2-(2-(*tert*-Butyldimethylsilyloxy)ethoxy)ethoxy)-ethoxy)benzofuran-2-yl)-*N*-methylpyridin-2-amine (5). **4** (61 mg, 0.17 mmol) and TBDMSCl (41 mg, 0.27 mmol) were dissolved in dichloromethane (10 mL) followed by imidazole (24 mg, 0.34 mmol). The solution was stirred at room temperature for 2 h. After a standard workup with ethyl acetate, the residue was purified by silica gel chromatography (hexane/ethyl acetate = 1:6) to give 73 mg of **5** (87.6%). ^{1}H NMR (400 MHz, $CDCl_3$): δ 0.08 (s, 6H), 0.90 (s, 9H), 2.98 (d, 3H, J = 5.2 Hz), 3.62 (d, 2H, J = 4.4 Hz), 3.70−3.74 (m, 6H), 3.84 (s, 2H), 4.11 (s, 2H), 5.18 (s, 1H), 6.47 (d, 1H, J = 8.8 Hz), 6.76 (s, 1H), 6.84 (dd, 1H, J_1 = 8.8 Hz, J_2 = 4.4 Hz), 7.00 (d, 1H, J = 2.4 Hz), 7.36 (d, 1H, J = 8.4 Hz), 7.87 (dd, 1H, J_1 = 8.8 Hz, J_2 = 2.4 Hz), 8.59 (d, 1H, J = 2.8 Hz). MS: m/z 487 ($M^+ + H$).

***tert*-Butyl 5-(5-(2-(2-(2-(*tert*-Butyldimethylsilyloxy)ethoxy)ethoxy)-2-benzofuranyl)-2-pyridinyl-(methyl)carbamate (6).** **5** (73 mg, 0.15 mmol) was dissolved in anhydrous THF (5.0 mL) followed by Boc anhydride (66 mg, 0.30 mmol). The solution was refluxed overnight. After a standard workup with ethyl acetate, the residue was purified by silica gel chromatography (hexane/ethyl acetate = 1:1) to give 37 mg of **6** (46.7%). ^{1}H NMR (400 MHz, $CDCl_3$): δ 0.03 (s, 6H), 0.86 (s, 9H), 1.50 (s, 9H), 3.37 (s, 3H), 3.62−3.68 (m, 6H), 3.82−3.88 (m, 2H), 4.09−4.12 (m, 2H), 6.86 (d, 1H, J = 4.4 Hz), 6.88 (s, 1H), 6.98 (d, 1H, J = 2.4 Hz), 7.33 (d, 1H, J = 8.8 Hz), 7.76 (d, 1H, J = 10.0 Hz), 7.95 (dd, 1H, J_1 = 8.8 Hz, J_2 = 2.4 Hz), 8.75 (d, 1H, J = 1.6 Hz). MS: m/z 587 ($M^+ + H$).

***tert*-Butyl 5-(5-(2-(2-(2-Hydroxyethoxy)ethoxy)ethoxy)-2-benzofuranyl)-2-pyridinyl(methyl)carbamate (7).** TBAF (1 M in THF, 0.30 mL) was added via a syringe to a solution of **6** (37 mg, 0.07 mL) in THF (5 mL). The solution was stirred at room temperature for 5 h. After a standard workup with ethyl acetate, the residue was purified by silica gel chromatography (hexane/ethyl acetate = 1:1) to give 31 mg of **7** (93.0%). ^{1}H NMR (400 MHz, $CDCl_3$): δ 1.57 (s, 9H), 3.45 (s, 3H), 3.62−3.65 (m, 2H), 3.70−3.78 (m, 6H), 3.83−3.93 (m, 2H), 4.07−4.18 (m, 2H), 6.87(d, 1H, J = 6.8 Hz), 6.94 (s, 1H), 7.06 (d, 1H, J = 2.4 Hz), 7.40 (d, 1H, J = 9.2 Hz), 7.82 (d, 1H, J = 8.8 Hz), 8.02 (dd, 1H, J_1 = 8.8 Hz, J_2 = 2 Hz), 8.83 (d, 1H, J = 2.8 Hz). MS: m/z 473 ($M^+ + H$).

2-(2-(2-(2-(6-(*tert*-Butoxycarbonyl)-3-pyridinyl)-5-benzo-furanyloxy)ethoxy)ethoxy)ethyl Methanesulfonate (8). **7** (30.5 mg, 0.065 mmol) was dissolved in dichloromethane (5 mL) followed by triethylamine (35 mg, 0.35 mmol). Methanesulfonyl chloride (25 mg, 0.21 mmol) was then added via a syringe. The solution was stirred at room temperature for 3 h. After a standard workup with ethyl acetate, the residue was purified by silica gel chromatography (hexane/ethyl acetate = 1:6) to give 25 mg of **8** (74.5%). ^{1}H NMR (400 MHz, $CDCl_3$): δ 1.54 (s, 9H), 3.06 (s, 3H), 3.44 (s, 3H), 3.69−3.72 (m, 6H), 3.79−3.88 (m, 2H), 4.11−4.17 (m, 2H), 4.37−4.39 (m, 2H), 6.90 (dd, 1H, J_1 = 9.2 Hz, J_2 = 2.8 Hz), 6.95 (s, 1H), 7.05 (d, 1H, J = 2.4 Hz), 7.40 (d, 1H, J = 8.8 Hz), 7.83 (d, 1H, J = 8.0 Hz), 8.02 (dd, 1H, J_1 = 8.8 Hz, J_2 = 2.4 Hz), 8.83 (d, 1H, J = 0.8 Hz). HRMS EI: m/z calcd for $C_{26}H_{34}N_2O_9S$ (M^+) 550.1985, found 550.1989.

***tert*-Butyl 5-(5-(2-(2-(2-Fluoroethoxy)ethoxy)ethoxy)-2-benzofuranyl)-2-pyridinyl(methyl)carbamate (9).** TBAF (1 M in THF, 0.20 mL) was added to a solution of **8** (27 mg, 0.05 mmol) in anhydrous THF (10 mL). The mixture was refluxed for 4 h. Afterward, it was cooled to room temperature. After a standard workup with ethyl acetate, the residue was purified by silica gel chromatography (hexane/ethyl acetate = 1:1) to give 22 mg of **9** (94.0%). ^{1}H NMR (400 MHz, $CDCl_3$): δ 1.57 (s, 9H), 3.44 (s, 3H), 3.71−3.83 (m, 6H), 3.88−3.91 (m, 2H), 4.22−4.51 (m, 1H), 4.61−4.63 (m, 1H), 6.91 (dd, 1H, J_1 = 8.8 Hz, J_2 = 2.4 Hz), 6.94 (s, 1H), 7.05 (d, 1H, J = 6.0 Hz), 7.38 (d, 1H, J = 8.8 Hz), 7.81 (d, 1H, J = 8.8 Hz), 8.02 (dd, 1H, J_1 = 8.8 Hz, J_2 = 2.4 Hz), 8.82 (d, 1H, J = 2.4 Hz). MS: m/z 475 ($M^+ + H$).

5-(5-(2-(2-(2-Fluoroethoxy)ethoxy)ethoxy)benzofuran-2-yl)-*N*-methylpyridin-2-amine (10). Trifluoroacetic acid (1.27 mL) was added slowly to a solution of **9** (22 mg, 0.047 mmol) in dichloromethane (2 mL). The mixture was then stirred at room temperature for 1 h. After a standard workup with ethyl acetate, the residue was purified by silica gel chromatography (hexane/ethyl acetate = 1:1) to give 9 mg of **10** (50.6%). ^{1}H NMR (400 MHz, $CDCl_3$): δ 2.98 (d, 3H, J = 5.2 Hz), 3.71−3.80 (m, 6H), 3.79−3.88 (m, 2H), 4.11−4.18 (m, 2H), 4.49−4.51 (m, 1H), 4.61−4.63 (m, 1H), 4.80 (s, 1H), 6.45 (d, 1H, J = 8.8 Hz), 6.75 (s, 1H), 6.85 (dd, 1H, J_1 = 8.8 Hz, J_2 = 2.4 Hz), 7.01 (d, 1H, J = 2.4 Hz), 7.36 (d, 1H, J = 9.2 Hz), 7.86 (dd, 1H, J_1 = 8.8 Hz, J_2 = 2.4 Hz), 8.59 (d, 1H, J = 2.0 Hz). HRMS (EI: m/z calcd for $C_{20}H_{23}FN_2O_4$ (M^+) 374.1642, found 374.1650.

5-Methoxy-2-(4-nitrophenyl)benzofuran (11). A solution of 2-hydroxy-5-methoxybenzaldehyde (1.22 g, 8.02 mmol), 4-nitrobenzyl bromide (1.73 g, 8.02 mmol), and K_2CO_3 (3.33 g, 24.06 mmol) in DMF (10 mL) was stirred under reflux overnight. The solvent was removed and the residue was recrystallized with ethyl acetate to give 1.39 g of **11** (64.0%). ^{1}H NMR (400 MHz, $CDCl_3$): δ 3.85 (s, 3H), 6.96−7.00 (m, 1H), 7.08 (d, 1H, J = 2.8 Hz), 7.18 (d, 1H, J = 2.8 Hz), 7.45 (d, 1H, J = 2.8 Hz), 7.95 (d, 2H, J = 8.8 Hz), 8.31 (d, 2H, J = 8.8 Hz).

5-Methoxy-2-(4-aminophenyl)benzofuran (12). A mixture of **11** (1.39 g, 5.16 mmol), $SnCl_2$ (5.82 g, 25.8 mmol), and ethanol (20 mL) was stirred under reflux for 2 h. After the mixture had cooled to room temperature, 1 M NaOH (20 mL) was added and extraction with ethyl acetate was carried out. The organic phase was dried over Na_2SO_4 and filtered. The filtrate was concentrated and the residue was purified by silica gel chromatography (hexane/ethyl acetate = 7:3) to give 609 mg of **12** (49.0%). ^{1}H NMR (400 MHz, $CDCl_3$): δ 3.85 (s, 3H), 6.71 (d, 2H, J = 8.8 Hz), 6.75 (s, 1H), 6.82 (dd, 1H, J_1 = 8.8 Hz, J_2 = 1.6 Hz), 6.97 (d, 1H, J = 2.8 Hz), 7.35 (d, 1H, J = 8.8 Hz), 7.65 (d, 2H, J = 8.8 Hz). MS: m/z 240 ($M^+ + H$).

5-Methoxy-2-(4-methylaminophenyl)benzofuran (13). A solution of NaOMe (5 M in MeOH, 4.0 mL) was added to a mixture of **12** (609 mg, 2.55 mmol) and paraformaldehyde (279 mg, 10.3 mmol) in methanol (30 mL) dropwise. The mixture was stirred under reflux for 1 h. After $NaBH_4$ (225 mg, 7.0 mmol) was added, the solution was heated under reflux for 2 h. Then 1 M NaOH (30 mL) was added to the cold mixture and extraction with $CHCl_3$ (30 mL) was conducted. The organic phase was dried over Na_2SO_4 and filtered. The solvent was removed, and the residue was purified by silica gel chromatography (hexane/ethyl acetate = 7:3) to give 616 mg of **13** (95.0%). ^{1}H NMR (400 MHz, $CDCl_3$): δ 2.84 (s, 3H), 3.85 (s, 3H), 6.71 (d, 2H, J = 8.8 Hz), 6.75 (s, 1H), 6.82 (dd, 1H, J_1 = 8.8 Hz, J_2 = 1.6 Hz), 6.97 (d, 1H, J = 2.8 Hz), 7.35 (d, 1H, J = 8.8 Hz), 7.65 (d, 2H, J = 8.8 Hz). MS: m/z 254 ($M^+ + H$).

5-Hydroxy-2-(4-methylaminophenyl)benzofuran (14). BBr_3 (12.4 mL, 1 M solution in CH_2Cl_2) was added to a solution of **13** (616 mg, 2.43 mmol) in CH_2Cl_2 (40 mL) dropwise in an ice bath. The mixture was allowed to warm to room temperature and stirred for 1 h. Water (20 mL) was added while the reaction mixture was cooled in an ice bath. The mixture was extracted with ethyl acetate, and the organic phase was dried over Na_2SO_4 and filtered. The filtrate was concentrated, and the residue was purified by silica gel chromatography (hexane/ethyl

acetate = 7:3) to give 576 mg of **14** (99.0%). ^{1}H NMR (400 MHz, $CDCl_3$): δ 2.92 (s, 3H), 3.92 (s, 1H), 6.64 (d, 2H, J = 8.4 Hz), 6.68 (s, 1H), 6.71 (dd, 1H, J_1 = 8.8 Hz, J_2 = 2.4 Hz), 6.93 (d, 1H, J = 2.4 Hz), 7.30 (d, 1H, J = 8.4 Hz), 7.70 (d, 2H, J = 8.4 Hz). MS: m/z 240 ($M^+ + H$).

2-(2-(2-(2-(4-(Methylamino)phenyl)benzofuran-5-yloxy)ethoxy)ethoxy)ethanol (15). To a solution of **14** (575 mg, 2.41 mmol) and 2-[2-(2-chloroethoxy)ethoxy]ethanol (810 μL, 8.91 mmol) in DMF (10 mL) was added anhydrous K_2CO_3 (1.23 g, 8.91 mmol). The reaction mixture was stirred for 18 h at 100 °C and then poured into water and extracted with chloroform. The organic layers were combined and dried over Na_2SO_4. Evaporation of the solvent afforded a residue, which was purified by silica gel chromatography (hexane/ethyl acetate = 1:6) to give 654 mg of **15** (73.2%). ^{1}H NMR (400 MHz, $CDCl_3$): δ 2.84 (s, 3H), 3.49−3.52 (m, 2H), 3.58−3.64 (m, 6H), 3.71−3.82 (m, 2H), 4.08−4.11 (m, 2H), 6.59 (d, 2H, J = 8.8 Hz), 6.65 (s, 1H), 6.77 (dd, 1H, J_1 = 8.8 Hz, J_2 = 2.8 Hz), 6.94 (d, 1H, J = 2.4 Hz), 7.26 (d, 1H, J = 8.8 Hz), 7.60 (d, 2H, J = 8.8 Hz). MS: m/z 486 ($M^+ + H$).

4-(5-(2-(2-(2-(*tert*-Butyldimethylsilyloxy)ethoxy)ethoxy)-ethoxy)benzofuran-2-yl)-*N*-methylbenzenamine (16). **15** (383 mg, 1.03 mmol) and TBDMSCl (243 mg, 1.61 mmol) were dissolved in dichloromethane (10 mL) followed by imidazole (142 mg, 2.06 mmol). The solution was stirred at room temperature for 4 h. After a standard workup with ethyl acetate, the residue was purified by silica gel chromatography (hexane/ethyl acetate = 1:1) to give 453 mg of **16** (90.6%). ^{1}H NMR (400 MHz, $CDCl_3$): δ 0.02 (s, 6H), 0.83 (s, 9H), 2.84 (s, 3H), 3.49−3.52 (m, 2H), 3.58−3.64 (m, 6H), 3.71−3.82 (m, 2H), 4.08−4.11 (m, 2H), 6.59 (d, 2H, J = 8.8 Hz), 6.65 (s, 1H), 6.77 (dd, 1H, J_1 = 8.8 Hz, J_2 = 2.8 Hz), 6.94 (d, 1H, J = 2.4 Hz), 7.26 (d, 1H, J = 8.8 Hz), 7.60 (d, 2H, J = 8.8 Hz). MS: m/z 486 ($M^+ + H$).

***tert*-Butyl 4-(5-(2-(2-(2-(*tert*-Butyldimethylsilyloxy)ethoxy)ethoxy)benzofuran-2-yl)phenyl-(methyl)carbamate (17).** Compound **16** (452 mg, 0.93 mmol) was dissolved in anhydrous THF (20 mL) followed by Boc anhydride (601 mg, 1.79 mmol). The solution was refluxed overnight. After standard workup with ethyl acetate, the residue was purified by silica gel chromatography (hexane/ethyl acetate = 7:3) to give 412 mg of **17** (75.6%). ^{1}H NMR (400 MHz, $CDCl_3$): δ 0.02 (s, 6H), 0.83 (s, 9H), 3.20 (s, 3H), 3.47−3.52 (m, 2H), 3.59−3.67 (m, 6H), 3.71−3.82 (m, 2H), 4.08−4.11 (m, 2H), 6.82 (d, 2H, J = 8.4 Hz), 6.95 (d, 1H, J = 3.6 Hz), 7.23 (d, 2H, J = 8.8 Hz), 7.29 (d, 1H, J = 8.4 Hz), 7.70 (d, 2H, J = 8.8 Hz). MS: m/z 586 ($M^+ + H$).

***tert*-Butyl 4-(5-(2-(2-(2-Hydroxyethoxy)ethoxy)ethoxy)-benzofuran-2-yl)phenyl(methyl)carbamate (18).** TBAF (1 M in THF, 1.83 mL) was added via a syringe to a solution of **17** (412 mg, 0.70 mL) in THF (10 mL). The solution was stirred at room temperature for 2 h. After a standard workup with ethyl acetate, the residue was purified by silica gel chromatography (hexane/ethyl acetate = 1:1) to give 324 mg of **18** (97.9%). ^{1}H NMR (400 MHz, $CDCl_3$): δ 1.40 (s, 9H), 3.18 (s, 3H), 3.49−3.53 (m, 2H), 3.58−3.66 (m, 6H), 3.74−3.79 (m, 2H), 6.82 (d, 2H, J = 8.4 Hz), 6.95 (d, 1H, J = 3.6 Hz), 7.22 (d, 2H, J = 8.8 Hz), 7.29 (d, 1H, J = 8.4 Hz), 7.70 (d, 2H, J = 8.8 Hz). MS: m/z 472 ($M^+ + H$).

2-(2-(2-(2-(4-(*tert*-Butoxycarbonyl)phenyl)benzofuran-5-yloxy)ethoxy)ethoxy)ethyl Methanesulfonate (19). **18** (324 mg, 0.688 mmol) was dissolved in dichloromethane (20 mL) followed by triethylamine (344 mg, 3.44 mmol). Methanesulfonyl chloride (237 mg, 2.06 mmol) was then added via a syringe. The solution was stirred at room temperature for 2 h. After a standard workup with ethyl acetate, the residue was purified by silica gel chromatography (hexane/ethyl acetate = 1:1) to give 374 mg of **19** (98.8%). ^{1}H NMR (400 MHz, $CDCl_3$): δ 1.47 (s, 9H), 3.02 (s, 3H), 3.26 (s, 3H), 3.63−3.72 (m, 6H), 3.79−3.82 (m, 2H), 4.32−4.35 (m, 2H), 6.86 (dd, 1H, J_1 = 8.8 Hz, J_2 = 2.4 Hz), 6.90 (s, 1H), 7.02 (d, 1H, J = 2.8 Hz), 7.30 (d, 2H, J = 8.8 Hz), 7.36 (d, 1H, J = 8.4 Hz), 7.76 (d, 2H, J = 8.8 Hz). HRMS EI: m/z calcd for $C_{27}H_{35}NO_9S$ (M^+) 549.6331, found 549.2025.

***tert*-Butyl 4-(5-(2-(2-(2-Fluoroethoxy)ethoxy)ethoxy)benzofuran-2-yl)phenyl(methyl)carbamate (20).** TBAF (1 M in THF, 0.50 mL) was added to a solution of **20** (55.3 mg, 0.10 mmol) in anhydrous THF (5 mL). The mixture was refluxed for 2 h and cooled to room temperature. After a standard workup with ethyl acetate, the residue was purified by silica gel chromatography (hexane/ethyl acetate = 1:1) to give 46 mg of **20** (97.2%). ^{1}H NMR (400 MHz, $CDCl_3$): δ 1.47 (s, 9H), 3.29 (s, 3H), 3.70−3.73 (m, 6H), 3.78−3.80 (m, 2H), 4.15−4.18 (m, 2H), 4.48−4.62 (m, 2H), 6.89−6.92 (m, 2H), 7.04 (d, 1H, J = 2.8 Hz), 7.30 (d, 2H, J = 8.8 Hz), 7.37 (d, 1H, J = 5.2 Hz), 7.79 (d, 2H, J = 8.8 Hz). MS: m/z 474 ($M^+ + H$).

4-(5-(2-(2-(2-Fluoroethoxy)ethoxy)ethoxy)benzofuran-2-yl)-*N*-methylbenzenamine (21). Trifluoroacetic acid (2.70 mL) was added slowly to a solution of **20** (46.0 mg, 0.10 mmol) in dichloromethane (3 mL). The mixture was then stirred at room temperature for 1 h. After a standard workup with ethyl acetate, the residue was purified by silica gel chromatography (hexane/ethyl acetate = 1:1) to give 16 mg of **21** (43.4%). ^{1}H NMR (400 MHz, $CDCl_3$): δ 2.88 (s, 3H), 3.72−3.75 (m, 6H), 3.87−3.89 (m, 2H), 4.05−4.11 (m, 2H), 4.49−4.63 (m, 2H), 6.65 (d, 2H, J = 8.8 Hz), 6.71 (s, 1H), 6.82 (dd, 1H, J_1 = 8.8 Hz, J_2 = 2.8 Hz), 7.00 (d, 1H, J = 2.4 Hz), 7.33 (d, 1H, J = 8.8 Hz), 7.66 (d, 2H, J = 8.8 Hz). HRMS EI: m/z calcd for $C_{21}H_{24}FNO_4$ (M^+) 373.4180, found 373.1683.

Binding Assays Using the Aggregated Aβ Peptides in Solution. Aβ(1−42) was purchased from Peptide Institute (Osaka, Japan). Aggregation was carried out by gently dissolving the peptide (0.25 mg/mL) in a buffer solution (pH 7.4) containing 10 mM sodium phosphate and 1 mM EDTA. The solution was incubated at 37 °C for 42 h with gentle and constant shaking. A mixture containing 50 μL of test compounds (0.008 pM to 400 μM in 10% EtOH), 50 μL of 0.02 nM [^{125}I]IMPY, 50 μL of Aβ(1−42) aggregates, and 850 μL of 10% EtOH was incubated at room temperature for 3 h. The mixture was then filtered through Whatman GF/B filters using a Brandel M-24 cell harvester, and the radioactivity of the filters containing the bound ^{125}I ligand was measured in a γ counter. Values for the half maximal inhibitory concentration (IC_{50}) were determined from displacement curves of three independent experiments using GraphPad Prism 5.0, and those for the inhibition constant (K_i) were calculated using the Cheng−Prusoff equation:[45] $K_i = IC_{50}/(1 + [L]/K_d)$, where [L] is the concentration of [^{125}I]IMPY used in the assay and K_d is the dissociation constant of IMPY (4.2 nM).

Radiolabeling with ^{18}F. [^{18}F]Fluoride was produced by cyclotron (CYPRIS HM-18, Sumitomo Heavy Industries, Tokyo) via an ^{18}O (p, n)^{18}F reaction and passed through a Sep-Pak Light QMA cartridge (Waters) as an aqueous solution in ^{18}O-enriched water. The cartridge was dried by N_2, and the ^{18}F activity was eluted with 1.0 mL of a Kryptofix 222/K_2CO_3 solution (9.5 mg of Kryptofix 222 and 1.7 mg of K_2CO_3 in acetonitrile/water (96/4)). The solvent was removed at 120 °C under a stream of argon gas. The residue was azeotropically dried with 1 mL of anhydrous acetonitrile twice at 120 °C under a stream of nitrogen gas. A solution of the mesylate precursors **8** and **19** (1.0 mg) in acetonitrile (200 μL) was added to the reaction vessel containing the ^{18}F activity. The mixture was heated at 120 °C for 5 min and was cooled for 1 min. HCl (10% aqueous solution, 450 μL) was then added, and the mixture was heated at 120 °C again for 5 min. An aqueous solution of NaOH was added to adjust the pH to 8−9. The mixture was extracted with ethyl acetate (1 mL × 2), and the solvent was removed under nitrogen gas. The residue was purified by preparative HPLC [YMC-Pack Pro C_{18} column (20 mm × 150 mm), acetonitrile/water (70/30), flow rate of 4.0 mL/min]. The retention time of the desired ^{18}F-labeled product is 13.3 min. The radiochemical purity and specific activity were determined by analytical HPLC [YMC-Pack Pro C_{18} column (4.6 mm × 150 mm), acetonitrile/water (50/50), flow rate of 1.0 mL/min], and [^{18}F]**10** and [^{18}F]**21** were obtained in a radiochemical purity of >99%

with a specific activity of 242 GBq/μmol. Specific activity was estimated by comparing the UV peak intensity of the purified ^{18}F-labeled compound with a reference nonradioactive compound of known concentration.

Biodistribution in Normal Mice. Experiments with animals were conducted in accordance with our institutional guidelines and approved by the Kyoto University Animal Care Committee. While under anesthesia with isoflurane, ddY mice (22−25 g, male) were injected directly into the tail vein with 100 μL of a 0.1% BSA solution containing [^{18}F]**10** and [^{18}F]**21** (185−370 kBq). The mice (n = 5 for each time point) were sacrificed at 2, 10, 30, and 60 min postinjection. The organs of interest were removed and weighed, and radioactivity was measured with an automatic γ counter (COBRAII, Packard). Percentage dose per organ was calculated by a comparison of the tissue counts to suitably diluted aliquots of the injected material. The % dose/g of samples was calculated by comparing the sample counts with the count of the diluted initial dose.

In Vitro Autoradiography Using Brain Sections from AD Patients. Post-mortem brain sections (5 μm, temporal lobe) of an AD patient and a control subject (5 μm, temporal lobe) were obtained from BioChain Institute Inc. They were incubated with [^{18}F]**10** and [^{18}F]**21** (444 kBq/50 μL) for 1 h at room temperature. The sections were then dipped in saturated Li_2CO_3 in 40% EtOH (two 2-min washes), washed with 40% EtOH (one 2-min wash), and rinsed with water for 30 s. After drying, the ^{18}F-labeled sections were exposed to a BAS imaging plate (Fuji Film, Tokyo, Japan) overnight. Autoradiographic images were obtained using a BAS5000 scanner system (Fuji Film).

Ex Vivo Autoradiography Using Tg2576 Mice. Tg2576 transgenic mice (36 months, male) and wild-type mice (36 months, male) were purchased from Taconic Farms, Inc. and used as an Alzheimer's model and an age-matched control, respectively. After anesthetization with 1% isoflurane, 11.1 MBq [^{18}F]**10** or [^{18}F]**21** in 200 μL of 0.1% BSA solution was injected through a tail vein. The animals were allowed to recover for 30 min and then killed by decapitation. The brains were immediately removed and frozen in dry ice/hexane bath. Sections of 20 μm were cut and exposed to a BAS imaging plate (Fuji Film, Tokyo, Japan) overnight. Ex vivo film autoradiograms were thus obtained. After autoradiographic examination, the same sections were stained by thioflavin-S to confirm the presence of Aβ plaques. For the staining of thioflavin-S, sections were immersed in a 0.125% thioflavin-S solution containing 50% EtOH for 3 min and washed in 50% EtOH. After drying, the sections were then examined using a microscope (Nikon, Eclipse 80i) equipped with a B-2A filter set (excitation, 450−490 nm; diachronic mirror, 505 nm; long-pass filter, 520 nm).

■ ASSOCIATED CONTENT

Supporting Information. Preparation for ^{18}F-labeling of **10** and **21**. This material is available free of charge via the Internet at http://pubs.acs.org.

■ AUTHOR INFORMATION

Corresponding Author

*For M.O.: phone, +81-75-753-4608; fax, +81-75-753-4568; e-mail, ono@pharm.kyoto-u.ac.jp. For H.S.: phone, +81-75-753-4556; fax, +81-75-753-4568, e-mail, hsaji@pharm.kyoto-u.ac.jp.

■ ACKNOWLEDGMENT

The study was supported by the Funding Program for Next Generation World-Leading Researchers and a Grant-in-Aid for Young Scientists (A) and Exploratory Research from the Ministry of Education, Culture, Sports, Science and Technology, Japan.

■ ABBREVIATIONS USED

AD, Alzheimer's disease; Aβ, β-amyloid; NFT, neurofibrillary tangle; PET, positron emission tomography; SB-13, 4-*N*-methylamino-4′-hydroxystilbene; PIB, 2-(4′-(methylaminophenyl)-6-hydroxybenzothiazole; FDDNP, 2-(1-(2-(*N*-(2-fluoroethyl)-*N*-methylamino)naphthalene-6-yl)ethylidene)malononitrile; FPHBF-1, 4-(5-(2-(2-(2-fluoroethoxy)ethoxy)ethoxy)benzofuran-2-yl)-*N*,*N*-dimethylbenzenamine; FPYBF-1, 5-(5-(2-(2-(2-fluoroethoxy)ethoxy)ethoxy)benzofuran-2-yl)-*N*,*N*-dimethylpyridin-2-amine; TBAF, tetra-*n*-butylammonium fluoride; THF, tetrahydrofuran; BOC, *tert*-butyloxycarbonyl; TBDMSCl, *tert*-butyldimethylsilyl chloride; IMPY, 2-(4′-dimethylaminophenyl)-6-iodoimidazo[1,2-*a*]pyridine

■ REFERENCES

(1) Hardy, J. A.; Higgins, G. A. Alzheimer's disease: the amyloid cascade hypothesis. *Science* **1992**, *256*, 184–185.

(2) Selkoe, D. J. Alzheimer's disease: genes, proteins, and therapy. *Physiol. Rev.* **2001**, *81*, 741–766.

(3) Selkoe, D. J. Imaging Alzheimer's amyloid. *Nat. Biotechnol.* **2000**, *18*, 823–824.

(4) Mathis, C. A.; Wang, Y.; Klunk, W. E. Imaging β-amyloid plaques and neurofibrillary tangles in the aging human brain. *Curr. Pharm. Des.* **2004**, *10*, 1469–1492.

(5) Nordberg, A. PET imaging of amyloid in Alzheimer's disease. *Lancet Neurol.* **2004**, *3*, 519–527.

(6) Ono, M.; Wilson, A.; Nobrega, J.; Westaway, D.; Verhoeff, P.; Zhuang, Z. P.; Kung, M. P.; Kung, H. F. ^{11}C-labeled stilbene derivatives as Aβ-aggregate-specific PET imaging agents for Alzheimer's disease. *Nucl. Med. Biol.* **2003**, *30*, 565–571.

(7) Verhoeff, N. P.; Wilson, A. A.; Takeshita, S.; Trop, L.; Hussey, D.; Singh, K.; Kung, H. F.; Kung, M. P.; Houle, S. In-vivo imaging of Alzheimer disease β-amyloid with [^{11}C]SB-13 PET. *Am. J. Geriatr. Psychiatry* **2004**, *12*, 584–595.

(8) Mathis, C. A.; Wang, Y.; Holt, D. P.; Huang, G. F.; Debnath, M. L.; Klunk, W. E. Synthesis and evaluation of ^{11}C-labeled 6-substituted 2-arylbenzothiazoles as amyloid imaging agents. *J. Med. Chem.* **2003**, *46*, 2740–2754.

(9) Klunk, W. E.; Engler, H.; Nordberg, A.; Wang, Y.; Blomqvist, G.; Holt, D. P.; Bergstrom, M.; Savitcheva, I.; Huang, G. F.; Estrada, S.; Ausen, B.; Debnath, M. L.; Barletta, J.; Price, J. C.; Sandell, J.; Lopresti, B. J.; Wall, A.; Koivisto, P.; Antoni, G.; Mathis, C. A.; Langstrom, B. Imaging brain amyloid in Alzheimer's disease with Pittsburgh compound-B. *Ann. Neurol.* **2004**, *55*, 306–319.

(10) Kudo, Y.; Okamura, N.; Furumoto, S.; Tashiro, M.; Furukawa, K.; Maruyama, M.; Itoh, M.; Iwata, R.; Yanai, K.; Arai, H. 2-(2-[2-Dimethylaminothiazol-5-yl]ethenyl)-6-(2-[fluoro]ethoxy)benzoxazole: a novel PET agent for in vivo detection of dense amyloid plaques in Alzheimer's disease patients. *J. Nucl. Med.* **2007**, *48*, 553–561.

(11) Johnson, A. E.; Jeppsson, F.; Sandell, J.; Wensbo, D.; Neelissen, J. A.; Jureus, A.; Strom, P.; Norman, H.; Farde, L.; Svensson, S. P. AZD2184: a radioligand for sensitive detection of β-amyloid deposits. *J. Neurochem.* **2009**, *108*, 1177–1186.

(12) Swahn, B. M.; Wensbo, D.; Sandell, J.; Sohn, D.; Slivo, C.; Pyring, D.; Malmstrom, J.; Arzel, E.; Vallin, M.; Bergh, M.; Jeppsson, F.; Johnson, A. E.; Jureus, A.; Neelissen, J.; Svensson, S. Synthesis and evaluation of 2-pyridylbenzothiazole, 2-pyridylbenzoxazole and 2-pyridylbenzofuran derivatives as ^{11}C-PET imaging agents for β-amyloid plaques. *Bioorg. Med. Chem. Lett.* **2010**, *20*, 1976–1980.

(13) Agdeppa, E. D.; Kepe, V.; Liu, J.; Flores-Torres, S.; Satyamurthy, N.; Petric, A.; Cole, G. M.; Small, G. W.; Huang, S. C.; Barrio, J. R. Binding characteristics of radiofluorinated 6-dialkylamino-2-naphthylethylidene derivatives as positron emission tomography imaging probes for β-amyloid plaques in Alzheimer's disease. *J. Neurosci.* **2001**, *21*, RC189.

(14) Shoghi-Jadid, K.; Small, G. W.; Agdeppa, E. D.; Kepe, V.; Ercoli, L. M.; Siddarth, P.; Read, S.; Satyamurthy, N.; Petric, A.; Huang, S. C.; Barrio, J. R. Localization of neurofibrillary tangles and β-amyloid plaques in the brains of living patients with Alzheimer disease. *Am. J. Geriatr. Psychiatry* **2002**, *10*, 24–35.

(15) Koole, M.; Lewis, D. M.; Buckley, C.; Nelissen, N.; Vandenbulcke, M.; Brooks, D. J.; Vandenberghe, R.; Van Laere, K. Whole-body biodistribution and radiation dosimetry of ^{18}F-GE067: a radioligand for in vivo brain amyloid imaging. *J. Nucl. Med.* **2009**, *50*, 818–822.

(16) Vandenberghe, R.; Van Laere, K.; Ivanoiu, A.; Salmon, E.; Bastin, C.; Triau, E.; Hasselbalch, S.; Law, I.; Andersen, A.; Korner, A.; Minthon, L.; Garraux, G.; Nelissen, N.; Bormans, G.; Buckley, C.; Owenius, R.; Thurfjell, L.; Farrar, G.; Brooks, D. J. ^{18}F-Flutemetamol amyloid imaging in Alzheimer disease and mild cognitive impairment: a phase 2 trial. *Ann. Neurol.* **2010**, *68*, 319–329.

(17) Nelissen, N.; Van Laere, K.; Thurfjell, L.; Owenius, R.; Vandenbulcke, M.; Koole, M.; Bormans, G.; Brooks, D. J.; Vandenberghe, R. Phase 1 study of the Pittsburgh compound B derivative ^{18}F-flutemetamol in healthy volunteers and patients with probable Alzheimer disease. *J. Nucl. Med.* **2009**, *50*, 1251–1259.

(18) Zhang, W.; Oya, S.; Kung, M. P.; Hou, C.; Maier, D. L.; Kung, H. F. F-18 polyethyleneglycol stilbenes as PET imaging agents targeting Aβ aggregates in the brain. *Nucl. Med. Biol.* **2005**, *32*, 799–809.

(19) Rowe, C. C.; Ackerman, U.; Browne, W.; Mulligan, R.; Pike, K. L.; O'Keefe, G.; Tochon-Danguy, H.; Chan, G.; Berlangieri, S. U.; Jones, G.; Dickinson-Rowe, K. L.; Kung, H. P.; Zhang, W.; Kung, M. P.; Skovronsky, D.; Dyrks, T.; Holl, G.; Krause, S.; Friebe, M.; Lehman, L.; Lindemann, S.; Dinkelborg, L. M.; Masters, C. L.; Villemagne, V. L. Imaging of amyloid β in Alzheimer's disease with ^{18}F-BAY94-9172, a novel PET tracer: proof of mechanism. *Lancet Neurol.* **2008**, *7*, 129–135.

(20) O'Keefe, G. J.; Saunder, T. H.; Ng, S.; Ackerman, U.; Tochon-Danguy, H. J.; Chan, J. G.; Gong, S.; Dyrks, T.; Lindemann, S.; Holl, G.; Dinkelborg, L.; Villemagne, V.; Rowe, C. C. Radiation dosimetry of β-amyloid tracers ^{11}C-PiB and ^{18}F-BAY94-9172. *J. Nucl. Med.* **2009**, *50*, 309–315.

(21) Zhang, W.; Kung, M. P.; Oya, S.; Hou, C.; Kung, H. F. ^{18}F-Labeled styrylpyridines as PET agents for amyloid plaque imaging. *Nucl. Med. Biol.* **2007**, *34*, 89–97.

(22) Choi, S. R.; Golding, G.; Zhuang, Z.; Zhang, W.; Lim, N.; Hefti, F.; Benedum, T. E.; Kilbourn, M. R.; Skovronsky, D.; Kung, H. F. Preclinical properties of ^{18}F-AV-45: a PET agent for Aβ plaques in the brain. *J. Nucl. Med.* **2009**, *50*, 1887–1894.

(23) Wong, D. F.; Rosenberg, P. B.; Zhou, Y.; Kumar, A.; Raymont, V.; Ravert, H. T.; Dannals, R. F.; Nandi, A.; Brasic, J. R.; Ye, W.; Hilton, J.; Lyketsos, C.; Kung, H. F.; Joshi, A. D.; Skovronsky, D. M.; Pontecorvo, M. J. In vivo imaging of amyloid deposition in Alzheimer disease using the radioligand ^{18}F-AV-45 (flobetapir F 18). *J. Nucl. Med.* **2010**, *51*, 913–920.

(24) Liu, Y.; Zhu, L.; Plossl, K.; Choi, S. R.; Qiao, H.; Sun, X.; Li, S.; Zha, Z.; Kung, H. F. Optimization of automated radiosynthesis of [^{18}F]AV-45: a new PET imaging agent for Alzheimer's disease. *Appl. Radiat. Isot.* **2010**, *68*, 2293–2297.

(25) Lin, K. J.; Hsu, W. C.; Hsiao, I. T.; Wey, S. P.; Jin, L. W.; Skovronsky, D.; Wai, Y. Y.; Chang, H. P.; Lo, C. W.; Yao, C. H.; Yen, T. C.; Kung, M. P. Whole-body biodistribution and brain PET imaging with [^{18}F]AV-45, a novel amyloid imaging agent—a pilot study. *Nucl. Med. Biol.* **2010**, *37*, 497–508.

(26) Clark, C. M.; Schneider, J. A.; Bedell, B. J.; Beach, T. G.; Bilker, W. B.; Mintun, M. A.; Pontecorvo, M. J.; Hefti, F.; Carpenter, A. P.; Flitter, M. L.; Krautkramer, M. J.; Kung, H. F.; Coleman, R. E.; Doraiswamy, P. M.; Fleisher, A. S.; Sabbagh, M. N.; Sadowsky, C. H.; Reiman, P. E.; Zehntner, S. P.; Skovronsky, D. M. Use of florbetapir-PET for imaging β-amyloid pathology. *J. Am. Med. Assoc.* **2011**, *305*, 275–283.

(27) Kung, H. F.; Choi, S. R.; Qu, W.; Zhang, W.; Skovronsky, D. ^{18}F stilbenes and styrylpyridines for PET imaging of Aβ plaques in Alzheimer's disease: a miniperspective. *J. Med. Chem.* **2010**, *53*, 933–941.

(28) Ono, M.; Kung, M. P.; Hou, C.; Kung, H. F. Benzofuran derivatives as Aβ-aggregate-specific imaging agents for Alzheimer's disease. *Nucl. Med. Biol.* **2002**, *29*, 633–642.

(29) Ono, M.; Kawashima, H.; Nonaka, A.; Kawai, T.; Haratake, M.; Mori, H.; Kung, M. P.; Kung, H. F.; Saji, H.; Nakayama, M. Novel benzofuran derivatives for PET imaging of β-amyloid plaques in Alzheimer's disease brains. *J. Med. Chem.* **2006**, *49*, 2725–2730.

(30) Cheng, Y.; Ono, M.; Kimura, H.; Kagawa, S.; Nishii, R.; Kawashima, H.; Saji, H. Fluorinated benzofuran derivatives for PET imaging of β-amyloid plaques in Alzheimer's disease brains. *ACS Med. Chem. Lett.* **2010**, *1*, 321–325.

(31) Ono, M.; Yoshida, N.; Ishibashi, K.; Haratake, M.; Arano, Y.; Mori, H.; Nakayama, M. Radioiodinated flavones for in vivo imaging of β-amyloid plaques in the brain. *J. Med. Chem.* **2005**, *48*, 7253–7260.

(32) Ono, M.; Haratake, M.; Mori, H.; Nakayama, M. Novel chalcones as probes for in vivo imaging of β-amyloid plaques in Alzheimer's brains. *Bioorg. Med. Chem.* **2007**, *15*, 6802–6809.

(33) Cheng, Y.; Ono, M.; Kimura, H.; Kagawa, S.; Nishii, R.; Saji, H. A novel ^{18}F-labeled pyridyl benzofuran derivative for imaging of β-amyloid plaques in Alzheimer's brains. *Bioorg. Med. Chem. Lett.* **2010**, *20*, 6141–6144.

(34) Miyaura, N.; Yamada, K.; Suzuki, A. A new stereospecific cross-coupling by the palladium-catalyzed reaction of 1-alkenylboranes with 1-alkenyl or 1-alkynyl halides. *Tetrahedron Lett.* **1979**, *36*, 3437–3440.

(35) Ono, M.; Haratake, M.; Saji, H.; Nakayama, M. Development of novel β-amyloid probes based on 3,5-diphenyl-1,2,4-oxadiazole. *Bioorg. Med. Chem.* **2008**, *16*, 6867–6872.

(36) Watanabe, H.; Ono, M.; Ikeoka, R.; Haratake, M.; Saji, H.; Nakayama, M. Synthesis and biological evaluation of radioiodinated 2,5-diphenyl-1,3,4-oxadiazoles for detecting β-amyloid plaques in the brain. *Bioorg. Med. Chem.* **2009**, *17*, 6402–6406.

(37) Kung, H. F.; Lee, C. W.; Zhuang, Z. P.; Kung, M. P.; Hou, C.; Plossl, K. Novel stilbenes as probes for amyloid plaques. *J. Am. Chem. Soc.* **2001**, *123*, 12740–12741.

(38) Ono, M.; Haratake, M.; Nakayama, M.; Kaneko, Y.; Kawabata, K.; Mori, H.; Kung, M. P.; Kung, H. F. Synthesis and biological evaluation of (*E*)-3-styrylpyridine derivatives as amyloid imaging agents for Alzheimer's disease. *Nucl. Med. Biol.* **2005**, *32*, 329–335.

(39) Ono, M.; Watanabe, R.; Kawashima, H.; Cheng, Y.; Kimura, H.; Watanabe, H.; Haratake, M.; Saji, H.; Nakayama, M. Fluoro-pegylated chalcones as positron emission tomography probes for in vivo imaging of β-amyloid plaques in Alzheimer's disease. *J. Med. Chem.* **2009**, *52*, 6394–6401.

(40) Maya, Y.; Ono, M.; Watanabe, H.; Haratake, M.; Saji, H.; Nakayama, M. Novel radioiodinated aurones as probes for SPECT imaging of β-amyloid plaques in the brain. *Bioconjugate Chem.* **2009**, *20*, 95–101.

(41) Hsiao, K.; Chapman, P.; Nilsen, S.; Eckman, C.; Harigaya, Y.; Younkin, S.; Yang, F.; Cole, G. Correlative memory deficits, Aβ elevation, and amyloid plaques in transgenic mice. *Science* **1996**, *274*, 99–102.

(42) Ono, M.; Hayashi, S.; Kimura, H.; Kawashima, H.; Nakayama, M.; Saji, H. Push−pull benzothiazole derivatives as probes for detecting β-amyloid plaques in Alzheimer's brains. *Bioorg. Med. Chem.* **2009**, *17*, 7002–7007.

(43) Ono, M.; Watanabe, R.; Kawashima, H.; Kawai, T.; Watanabe, H.; Haratake, M.; Saji, H.; Nakayama, M. ^{18}F-Labeled flavones for in vivo imaging of β-amyloid plaques in Alzheimer's brains. *Bioorg. Med. Chem.* **2009**, *17*, 2069–2076.

(44) Toyama, H.; Ye, D.; Ichise, M.; Liow, J. S.; Cai, L.; Jacobowitz, D.; Musachio, J. L.; Hong, J.; Crescenzo, M.; Tipre, D.; Lu, J. Q.; Zoghbi, S.; Vines, D. C.; Seidel, J.; Katada, K.; Green, M. V.; Pike, V. W.; Cohen, R. M.; Innis, R. B. PET imaging of brain with the β-amyloid probe, [^{11}C]6-OH-BTA-1, in a transgenic mouse model of Alzheimer's disease. *Eur. J. Nucl. Med. Mol. Imaging* **2005**, *32*, 593–600.

(45) Cheng, Y.; Prusoff, W. Relationship between the inhibition constant (K1) and the concentration of inhibitor which causes 50% inhibition (I50) of an enzymatic reaction. *Biochem. Pharmacol.* **1973**, *22*, 3099–3108.

(46) Leo, A. J. Calculating log P_{oct} from structures. *Chem. Rev.* **1993**, *93*, 1281–1306.

Journal of Medicinal Chemistry

ARTICLE

pubs.acs.org/jmc

Synthesis and Structure−Affinity Relationships of Novel Dibenzylideneacetone Derivatives as Probes for β-Amyloid Plaques

Mengchao Cui,[†,‡] Masahiro Ono,[*,†] Hiroyuki Kimura,[†] Boli Liu,[‡] and Hideo Saji[*,†]

[†]Graduate School of Pharmaceutical Sciences, Kyoto University, 46-29 Yoshida Shimoadachi-cho, Sakyo-ku, Kyoto 606-8501, Japan

[‡]Key Laboratory of Radiopharmaceuticals, Ministry of Education, College of Chemistry, Beijing Normal University, Beijing 100875, People's Republic of China

Supporting Information

ABSTRACT: A new and extensive set of dibenzylideneacetone derivatives was synthesized and screened for affinity toward $A\beta_{1-42}$ aggregates. Structure−activity relationships revealed the binding of dibenzylideneacetones to be affected by various substituents. The introduction of a substituent group in the ortho position reduced or abolished the binding. However, the para position was highly tolerant of sterically demanding substitutions. Three radioiodinated ligands (**6**, **70**, and **71**) and two ^{18}F fluoropegylated (FPEG) ligands (**83** and **85**) were prepared, all of which displayed high affinity for $A\beta_{1-42}$ aggregates (K_i ranging from 0.9 to 7.0 nM). In biodistribution experiments, they exhibited good initial penetration (1.59, 4.68, 4.56, 4.13, and 5.15% ID/g, respectively, at 2 min) of and fast clearance from the brain. Autoradiography with sections of postmortem AD brain and transgenic mouse brain confirmed the high affinity of these tracers. These preliminary results strongly suggest the dibenzylideneacetone structure to be a potential new scaffold for β-amyloid imaging probes.

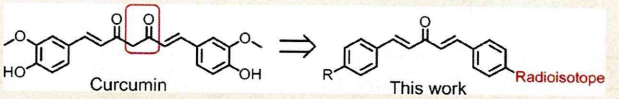

INTRODUCTION

Alzheimer's disease (AD) is an irreversible, progressive brain disorder that accounts for the majority of dementia cases. Histopathologically, AD is characterized by β-amyloid ($A\beta$) plaques composed mainly of mis-folded $A\beta$ peptides and neurofibrillary tangles (NFTs) containing hyperphosphorylated τ protein.[1,2] However, the precise molecular mechanisms leading to AD remain unknown. Several theories have arisen, with the amyloid cascade hypothesis perhaps the most prominent.[3,4] Moreover, a refined version of the amyloid cascade hypothesis proposes that soluble $A\beta$ peptides (soluble oligomers or protofibrils), not mature $A\beta$ plaques, exert toxic effects on neuronal cells.[5,6] The clinical diagnosis of AD is primarily based on neurological observations and patient history and is often difficult and unreliable. Although there is a lack of correlation between cognitive decline and elevated levels of $A\beta$ plaques in the brain,[7,8] several reports indicate that overaccumulation of $A\beta$ peptides initiates a sequence of events that lead to neurodegeneration.[9,10] Therefore, $A\beta$ plaques could be considered a biomarker for the early diagnosis of AD.

With the assistance of nuclear imaging techniques such as positron emission tomography (PET) and single photon emission computed tomography (SPECT), radionuclide-labeled agents targeting $A\beta$ plaques in the brain may greatly facilitate the diagnosis of AD.[11,12] Over the past 10 years, several agents for imaging $A\beta$ plaques have been tested in humans (Figure 1). Pittsburgh compound B, 2-(4′-[^{11}C]methylaminophenyl)-6-hydroxybenzothiazole ([^{11}C]PIB), is, to date, the most widely used PET radioligand for amyloid imaging[13,14] and clearly distinguishes between AD and control cases. However, the short half-life of carbon-11 (20.4 min) limits the potential clinical use of this agent. Great efforts have been made to develop imaging agents labeled with a longer half-life isotope, fluorine-18 (109.4 min). An analogue of PIB, [^{18}F]-2-(3-fluoro-4-(methylamino)phenyl) benzo[*d*]thiazol-6-ol ([^{18}F]GE-067),[15] and the stilbene derivatives [^{18}F]-4-(*N*-methylamino)-4′-(2-(2-(2-fluoroethoxy)ethoxy) ethoxy)-stilbene ([^{18}F]BAY94-9172)[16] and [^{18}F]-(*E*)-4-(2-(6-(2-(2-(2-fluoroethoxy)ethoxy)ethoxy)pyridin-3-yl)vinyl)-*N*-methylaniline ([^{18}F]AV-45)[17,18] are under commercial development for the mapping of $A\beta$ plaque burden in living brain tissue. In addition, [^{123}I]-6-iodo-2-(4′-dimethylamino-)phenyl-imidazo [1,2]pyridine ([^{123}I]IMPY)[19−21] is the first SPECT probe to be evaluated in humans. The preliminary clinical data showed a poor signal-to-noise ratio, making it difficult to distinguish AD patients. Currently, some research groups have continued to develop more useful probes for the SPECT imaging of cerebral $A\beta$ plaques.[22−24]

Almost all of the agents evaluated in humans have been developed based on thioflavin T (ThT) and Congo Red (CR), dyes used for $A\beta$ plaques in sections of AD brain. $A\beta$ plaques are known to have various binding sites for ligands,[25] and numerous $A\beta$-binding compounds besides ThT and CR derivatives have been reported. The application of these new compounds to PET/SPECT imaging should contribute to the development of new probes with improved properties including higher affinity for $A\beta$ plaques and less nonspecific binding in the white matter of the brain. Indeed, we have found that flavonoids such as

Received: October 28, 2010
Published: March 21, 2011

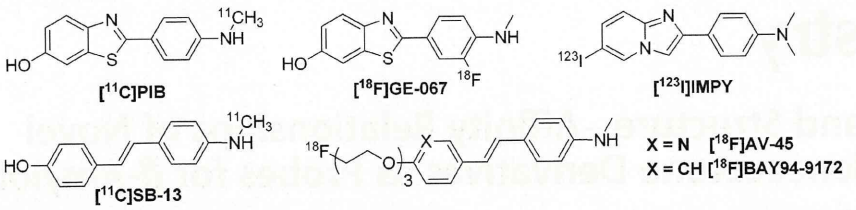

Figure 1. Chemical structure of Aβ imaging probes used in clinical trials.

Scheme 1[a]

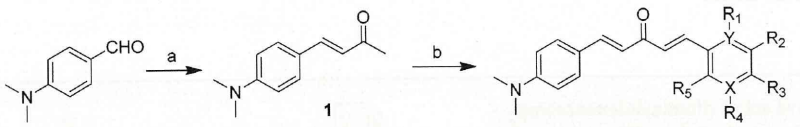

Compound	R_1	R_2	R_3	R_4	R_5	X	Y	Yield
2	H	H	H	H	H	CH	CH	31.6%
3	H	H	F	H	H	CH	CH	77.3%
4	H	H	Cl	H	H	CH	CH	78.5%
5	H	H	Br	H	H	CH	CH	49.4%
6	H	H	I	H	H	CH	CH	61.5%
7	H	H	OH	H	H	CH	CH	19.5%
8	H	H	OCH_3	H	H	CH	CH	71.3%
9	H	H	NO_2	H	H	CH	CH	64.3%
10	H	H	NH_2	H	H	CH	CH	11.5%
11	H	H	$NHCH_3$	H	H	CH	CH	6.2%
12	H	H	$N(CH_3)_2$	H	H	CH	CH	32.2%
13	H	H	COOH	H	H	CH	CH	2.5%
14	H	H	CF_3	H	H	CH	CH	79.9%
15	H	H	CH_3	H	H	CH	CH	84.5%
16	H	H	$N(Et)_2$	H	H	CH	CH	46.2%
17	H	H	$N(Ph)_2$	H	H	CH	CH	41.7%
18	H	H	OBn	H	H	CH	CH	27.4%
19	H	F	H	H	H	CH	CH	63.4%
20	H	Br	H	H	H	CH	CH	77.5%
21	H	I	H	H	H	CH	CH	57.3%
22	H	NO_2	H	H	H	CH	CH	39.4%
23	H	NH_2	H	H	H	CH	CH	40.9%
24	H	$NHCH_3$	H	H	H	CH	CH	30.0%
25	H	$N(CH_3)_2$	H	H	H	CH	CH	28.4%

Compound	R_1	R_2	R_3	R_4	R_5	X	Y	Yield
26	OBn	H	H	H	H	CH	CH	51.0%
27	Cl	H	H	H	H	CH	CH	78.5%
28	OH	H	H	H	H	CH	CH	37.2%
29	NO_2	H	H	H	H	CH	CH	35.8%
30	NH_2	H	H	H	H	CH	CH	41.4%
31	$NHCH_3$	H	H	H	H	CH	CH	82.4%
32	Cl	H	H	H	Cl	CH	CH	6.3%
33	Cl	H	H	H	F	CH	CH	62.5%
34	H	CF_3	H	CF_3	H	CH	CH	21.3%
35	H	OCH_3	OCH_3	H	H	CH	CH	40.8%
36	H	OCH_3	H	OCH_3	H	CH	CH	70.4%
37	OCH_3	H	OCH_3	H	H	CH	CH	71.4%
38	H	OCH_3	OCH_3	OCH_3	H	CH	CH	71.6%
39	OCH_3	H	OCH_3	H	OCH_3	CH	CH	58.8%
40	H	OCH_3	OBn	H	H	CH	CH	61.6%
41	OH	H	H	Br	H	CH	CH	15.0%
42	H	OPh	H	H	H	CH	CH	83.9%
43	OBn	H	H	NO_2	H	CH	CH	83.3%
44	H	H	$OC(Ph)_3$	H	H	CH	CH	40.6%
45	H	H	Cl	H	H	N	CH	84.7%
46	H	H	Br	H	H	N	CH	67.7%
47	H	H	I	H	H	N	CH	32.5%
48	H	H	H	H	H	CH	N	56.5%

[a] Reagents and conditions: (a) NaOH (1 M), acetone, room temperature. (b) NaOMe (28% in MeOH), EtOH, substituted benzaldehyde, room temperature. (c) $SnCl_2$, EtOH, HCl, reflux. (d) K_2CO_3, CH_3I, room temperature.

flavone,[26,27] chalcone,[28,29] and aurone[30,31] strongly bind to Aβ plaques and applied them as new PET/SPECT probes (Figure 2). However, there is still a need for novel molecular scaffolds to serve in smart Aβ probes. Furthermore, many basic scientific questions regarding how these small organic molecular probes attach to amyloid fibrils remain to be answered. Elucidation of the mode of binding between Aβ aggregates and small ligands may enable the rational molecular design of more useful imaging probes in the future.

In 2006, Ryu et al. reported a [^{18}F]-fluoropropyl-substituted curcumin derivative, 1-[4-(3-[^{18}F]fluoropropoxy)-3-methoxyphenyl]-5-hydroxy-7-(4-hydroxy-3-methoxyphenyl)-1,4,6-heptatrien-3-one, as a specific Aβ probe with high affinity (0.07 nM using [^{125}I]-1-iodo-2,5-bis(3-hydroxycarbonyl-4-methoxy)styrylbenzene ([^{125}I]IMSB) as the radiolabeled standard). However, its poor penetration of the brain together with instability in vivo hampered its potential clinical use (0.52% ID/g at 2 min and 0.11% ID/g at 30 min). Studies indicated that this derivative was quickly converted to an unidentified polar product, which cannot cross the blood–brain barrier (BBB).[32] Several papers demonstrated that the β-diketone moiety (methylene moiety) in the middle of curcumin's structure is responsible for the instability and poor pharmacokinetic profile under physiological conditions.[33] In addition, the decomposition of curcumin can occur as a result of exposure to light, a process also mediated by the active methylene moiety.[34,35]

To improve the pharmacokinetic profile of curcumin, modifications to the middle of the compound that lead to a dibenzylideneacetone structure lacking an active methylene

moiety and one carbonyl moiety but maintaining the two aromatic rings responsible for the binding of Aβ plaques were explored. Such dibenzylideneacetone derivatives can be simply obtained by a one-pot reaction.

In the present study, a series of dibenzylideneacetones with various substitutents were synthesized and screened for Aβ binding. We examined the possible structure−activity relationship (SAR) of these analogues using substitutions on the aryl rings, believing the SAR results would allow for a more rational design of ligands. Three radioiodinated and two ^{18}F FPEG (fluoro-pegylated) derivatives with high affinity for Aβ aggregates were evaluated in vitro and in vivo as potential probes for PET or SPECT.

Scheme 2[a]

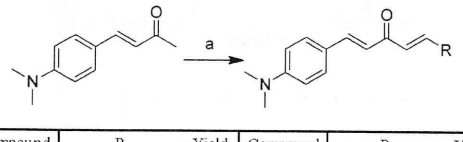

Compound	R	Yield	Compound	R	Yield
49		3.3%	54		71.9%
50		83.9%	55		12.6%
51		47.0%	56	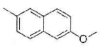	43.8%
52		71.0%	57		10.2%
53	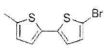	72.1%			

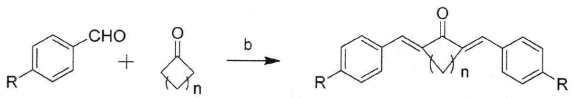

Compound	R	n	Yield
58	H	0	15.7%
59	Cl	0	67.2%
60	OCH_3	0	53.8%
61	H	3	88.3%
62	Cl	3	71.2%
63	OCH_3	3	74.3%
64	$N(CH_3)_2$	3	12.3%

[a] Reagents and conditions: (a) NaOMe (28% in MeOH), EtOH, substituted aromatic aldehyde, room temperature. (b) NaOMe (28% in MeOH), EtOH, room temperature.

RESULTS AND DISCUSSION

Chemistry and Radiochemistry. The core structure of the dibenzylideneacetones was produced as shown in Schemes 1−3. The key step was the base-catalyzed Claisen condensation reaction starting from suitably substituted aromatic aldehydes and aliphatic ketones. The unsymmetrical dibenzylideneacetones (**2**−**9**, **12**−**22**, **26**−**29**, **32**−**57**, and **68**−**71**) were obtained in 3−85% yields, and the symmetric compounds (**58**−**64**) were obtained in 12−88% yields. The amino-substituted compounds **10**, **23**, **30**, and **66** were produced by reducing the nitro group using $SnCl_2$. Subsequent methylation of the amino group using methyl iodide afforded mono- or dimethylated derivatives (**11**, **24**, **25**, **31**, and **67**). The tributyltin precursors (**72**−**74**) were prepared from the corresponding bromo compounds (**5**, **68**, and **69**) in a bromo to tributyltin exchange reaction catalyzed by $(Ph_3P)_4Pd$ (yield, 22.9−30.2%). The FPEG dibenzylideneacetones **81**−**83** and **85** were prepared by the procedures shown in Schemes 4 and 5. To prepare compounds with different numbers of ethoxy units as the linkage, the dimethylated derivative **1** or monomethylated derivative **67** was coupled with the polyethyleneglycol-modified benzaldhyde to obtain **75**−**77** and **86**, respectively. For the dimethylated dibenzylideneacetone, tosylation of the free hydroxyl groups present in **75**−**77** afforded the precursor **78**−**80**, which readily reacted with anhydrous tetra-*n*-butylammonium fluoride (TBAF) at reflux to give the "cold" FPEG dibenzylideneacetones, **81**−**83** (Scheme 4). For the monomethylated dibenzylideneacetone, the hydroxy group in **86** was subsequently protected with *tert*-butyldimethylsilyl chloride (TBDMSCl) to give the TBS-protected compound **87**. Compound **88** was obtained by protecting the methylamino group of **87** with

Scheme 3[a]

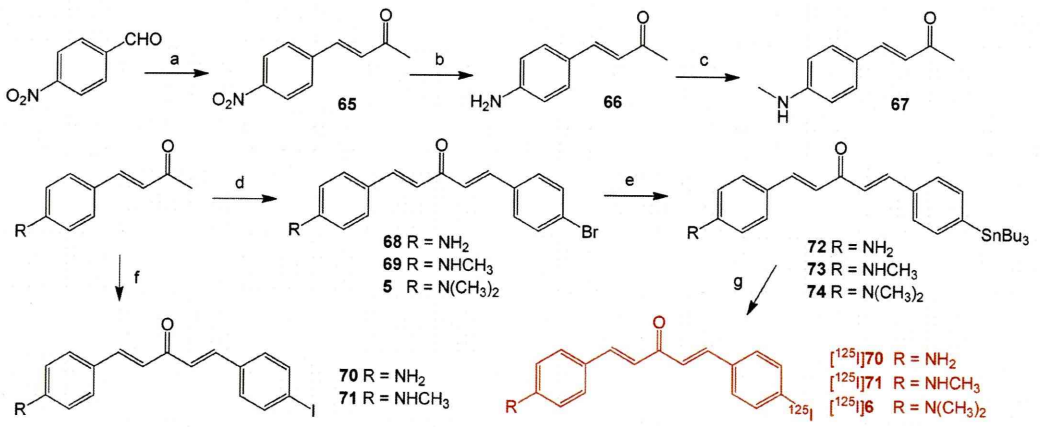

[a] Reagents and conditions: (a) (1) K_2CO_3, acetone, room temperature; (2) HCl, room temperature. (b) $SnCl_2$, EtOH, HCl, reflux. (c) K_2CO_3, CH_3I, room temperature. (d) NaOMe (28% in MeOH), EtOH, 4-bromobenzaldehyde, room temperature. (e) $(Bu_3Sn)_2$, $(Ph_3P)_4Pd$, toluene, reflux. (f) NaOMe (28% in MeOH), EtOH, 4-iodobenzaldehyde, room temperature. (g) [^{125}I]NaI, HCl (1 M), H_2O_2 (3%).

dx.doi.org/10.1021/jm101404k |J. Med. Chem. 2011, 54, 2225–2240

Scheme 4[a]

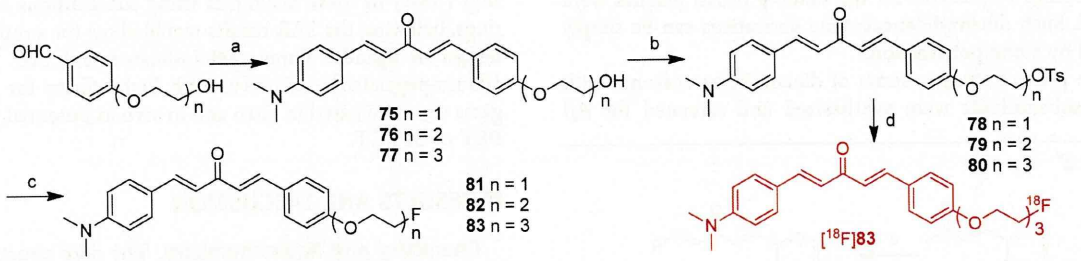

[a] Reagents and conditions: (a) NaOMe (28% in MeOH), EtOH, **1**, room temperature. (b) TsCl, pyridine, room temperature. (c) THF, TBAF (1 M), reflux. (d) K_{222}, $[^{18}F]^-$, DMSO, 120 °C.

Scheme 5[a]

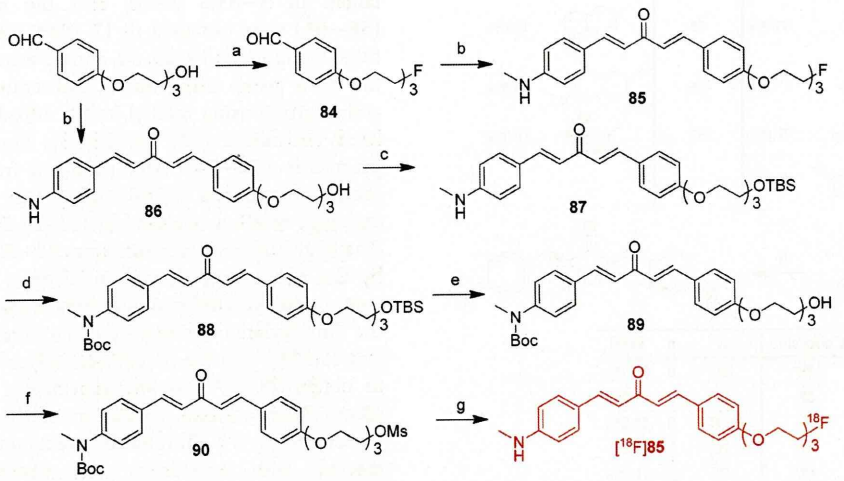

[a] Reagents and conditions: (a) DAST, $CHCl_3$, −78 °C. (b) NaOMe (28% in MeOH), EtOH, **67**, room temperature. (c) TBDMSCl, imidazole, DCM, room temperature. (d) $(BOC)_2O$, THF, reflux. (e) THF, TBAF (1 M), reflux. (f) MsCl, Et_3N, DCM, room temperature. (g) (1) K_{222}, $[^{18}F]^-$, DMSO, 120 °C; (2) HCl (1 M), 120 °C.

butyloxycarbonyl (BOC). After removal of the TBS-protecting group of **88** with TBAF, the free hydroxyl group was converted into mesylates by reacting with methanesulfonyl chloride in the presence of triethylamine to give **89**. The "cold" fluorinated compound **85** was successfully obtained by stirring **67** and the FPEG benzaldhyde **84** in ethanol (Scheme 5).

The radioiodinated ligands $[^{125}I]$**6**, **70**, and **71** were prepared from the corresponding tributyltin precursors through an iododestannylation reaction using hydrogen peroxide as an oxidant with radiochemical yield of 27.6, 15.3, and 24.1%, respectively (Scheme 3). After purification by high-performance liquid chromatography (HPLC), the radiochemical purity of these radiotracers was greater than 98%. The specific activity of the no carrier-added preparation was comparable to that of $Na^{125}I$, 2200 Ci/mmol. Finally, the radiochemical identities of $[^{125}I]$**6**, **70**, and **71** were verified using HPLC by coinjection with the nonradioactive compounds. To make the desired ^{18}F-labeled dibenzylideneacetone $[^{18}F]$**83**, the tosylate precursor **80** was mixed with $[^{18}F]$fluoride/potassium carbonate and Kryptofix 222 in dimethyl sulfoxide (DMSO) under heating at 120 °C for 5 min. The mixture was loaded on a Sep-Pak Plus-C18 cartridge (Waters), and the elution was purified by HPLC (radiochemical purity >98%, radiochemical yield 49%, decay corrected). For $[^{18}F]$**85**, the *N*-BOC-protected mesylate **90** was employed as the precursor. After 5 min at 120 °C, the mixture was treated with aqueous HCl to remove the *N*-BOC-protecting group. The crude product was purified by HPLC (radiochemical purity >98%, radiochemical yield 13%, decay corrected).

SAR Analysis. The affinity of these dibenzylideneacetone derivatives (**2**−**64**, **70**, **71**, **81**−**83**, and **85**) for $A\beta_{1-42}$ aggregates was examined with competition binding assays using $[^{125}I]$IMPY as the competing radioligand. IMPY and curcumin were also screened using the same system for comparison. The results are listed in Table 1. Dibenzylideneacetone (**58**) without any substituents showed moderate affinity (K_i = 242.5 ± 42.8 nM). Introducing Cl or methoxy groups at the para position on both phenyl rings to form symmetrical ligands increased the binding (e.g., **59**, K_i = 9.0 ± 1.2 nM; **60**, K_i = 6.5 ± 1.2 nM), especially for **12** with two *N*,*N*-dimethylamino groups (K_i = 2.7 ± 0.6 nM), whose affinity increased about 90-fold. As compared with **58**, **61** with a cyclohexanone spacer in the middle showed a decrease in affinity (K_i = 704.3 ± 90.3 nM). A comparable increase in binding was also observed on introducing Cl (**62**, K_i = 11.4 ± 0.8 nM), methoxy (**63**, K_i = 24.8 ± 2.5 nM), or *N*,*N*-dimethylamino (**64**, K_i = 1.0 ± 0.3 nM) groups for these symmetrical dibenzylidenecyclohexanones. These observations demonstrated again that the *N*,*N*-dimethylamino moiety plays a critical role in maintaining affinity for Aβ aggregates.

Table 1. Inhibition Constants (K_i, nM) for Binding to Aggregates of Aβ_{1-42} versus [^{125}I]IMPY

compound	K_i (nM)[a]	compound	K_i (nM)[a]	compound	K_i (nM)[a]
2	1.2 ± 0.2	**26**	18.6 ± 8.1	**50**	8.5 ± 0.8
3	3.7 ± 0.9	**27**	0.9 ± 0.1	**51**	5.3 ± 0.5
4	1.1 ± 0.2	**28**	28.2 ± 5.1	**52**	3.8 ± 0.4
5	2.8 ± 0.5	**29**	18.8 ± 3.0	**53**	11.7 ± 1.1
6	0.9 ± 0.2	**30**	8.4 ± 3.0	**54**	1.8 ± 0.2
7	6.8 ± 1.6	**31**	2636.5 ± 140.8	**55**	4.2 ± 0.4
8	0.7 ± 0.1	**32**	18.5 ± 0.9	**56**	2.5 ± 0.2
9	5.2 ± 1.1	**33**	9.2 ± 1.0	**57**	21.1 ± 1.2
10	3.7 ± 0.4	**34**	4.0 ± 0.5	**58**	242.5 ± 42.8
11	2.9 ± 0.5	**35**	5.4 ± 0.9	**59**	9.0 ± 1.2
12	2.7 ± 0.6	**36**	4.7 ± 2.1	**60**	6.5 ± 1.2
13	78.1 ± 8.5	**37**	2.8 ± 0.8	**61**	704.3 ± 90.3
14	0.8 ± 0.2	**38**	5.2 ± 0.6	**62**	11.4 ± 0.8
15	1.3 ± 0.2	**39**	39.1 ± 4.8	**63**	24.8 ± 2.5
16	15.7 ± 3.9	**40**	4.1 ± 0.4	**64**	1.0 ± 0.3
17	131.2 ± 20.3	**41**	16.2 ± 5.1	**70**	7.0 ± 2.2
18	2.0 ± 0.2	**42**	3.8 ± 1.1	**71**	2.8 ± 0.5
19	1.2 ± 0.1	**43**	33.3 ± 3.8	**81**	5.6 ± 2.5
20	1.9 ± 0.3	**44**	2.8 ± 0.4	**82**	4.4 ± 1.3
21	5.5 ± 1.7	**45**	2.2 ± 0.3	**83**	6.9 ± 1.4
22	4.0 ± 1.4	**46**	2.3 ± 0.1	**85**	8.6 ± 1.3
23	13.7 ± 3.4	**47**	4.8 ± 1.3	IMPY	10.5 ± 1.0
24	8.1 ± 1.4	**48**	23.0 ± 1.6	curcumin	49.8 ± 8.0
25	8.0 ± 0.6	**49**	5.8 ± 1.2		0.20 ± 0.06[b]

[a] Measured in triplicate with results given as the mean ± SD. [b] Data from ref 32.

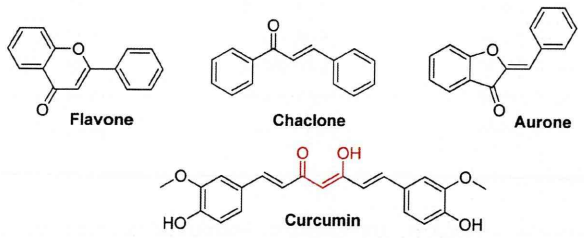

Figure 2. New backbone structures as Aβ imaging probes.

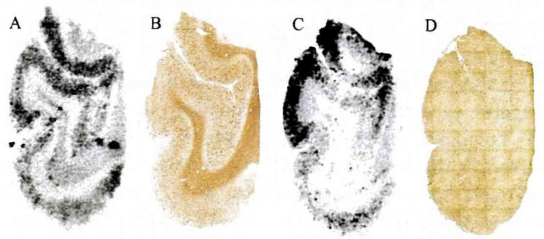

Figure 3. Autoradiography of [^{125}I]**6** and [^{125}I]**70** in vitro in AD brain sections (temporal lobe) (A and C). The presence and distribution of plaques in the sections were confirmed with immunohistochemical staining using a monoclonal Aβ antibody (B and D).

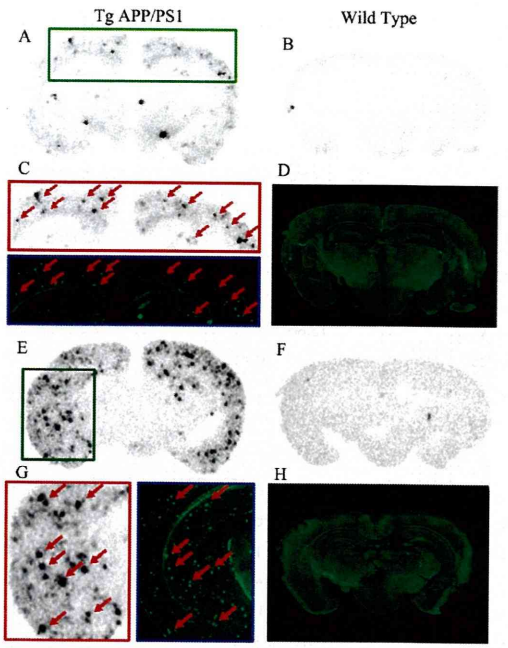

Figure 4. Autoradiography of [^{18}F]**83** and [^{18}F]**85** in vitro in Tg model mouse (C57BL6-APP/PS1, 12 months old, male) brain sections (A and E) and control sections (B and F). The presence and distribution of plaques in the sections were confirmed with thioflavin-S (C and G). Arrows show the correspondence to Aβ plaques.

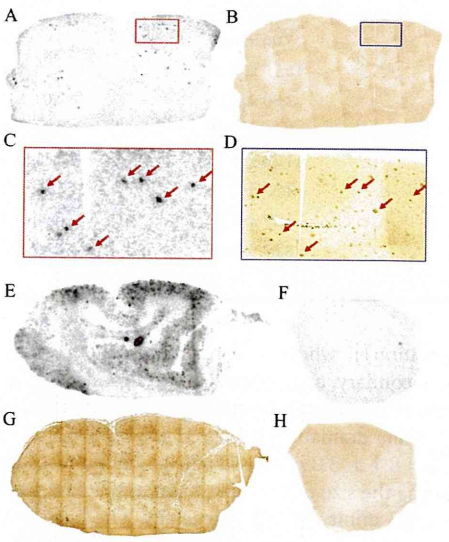

Figure 5. Autoradiography of [^{18}F]**83** and [^{18}F]**85** in vitro in AD brain sections and control sections (temporal lobe) (A, C, E, and F). The presence and distribution of plaques in the sections were confirmed with immunohistochemical staining using a monoclonal Aβ antibody (B, D, and G).

An extensive set of unsymmetrical dibenzylideneacetones with a *N,N*-dimethylamino group were synthesized. In general, the methylation of a primary amino group to form a secondary amino or tertiary amino group increased the affinity [e.g., **6** > **71** > **70** (para position); **12** > **11** > **10** (para position); **25** > **24** > **23**

Table 2. Biodistribution of in ddY Normal Mice after iv Injections of [^{125}I]Tracers (% ID/g, Mean ± SD, n = 4)

organ	2 min	15 min	30 min	60 min	120 min
		[^{125}I]**6** (Log D = 3.66 ± 0.09)			
blood	11.62 ± 1.22	6.58 ± 2.15	3.98 ± 0.28	2.16 ± 0.55	2.29 ± 0.65
brain	1.59 ± 0.04	1.11 ± 0.28	0.63 ± 0.03	0.28 ± 0.03	0.26 ± 0.07
heart	6.42 ± 0.80	2.69 ± 0.85	1.62 ± 0.20	1.03 ± 0.24	1.19 ± 0.17
liver	44.64 ± 6.19	32.80 ± 5.01	24.64 ± 2.85	11.54 ± 0.60	16.47 ± 1.38
spleen	11.59 ± 1.10	9.94 ± 2.07	12.26 ± 3.95	6.28 ± 2.87	7.34 ± 0.67
lung	24.45 ± 1.67	12.97 ± 3.05	6.91 ± 1.32	3.64 ± 0.47	3.35 ± 0.12
kidney	15.86 ± 1.37	22.23 ± 5.52	15.63 ± 1.71	7.00 ± 2.62	8.55 ± 1.98
stomach[a]	1.16 ± 0.15	1.75 ± 0.15	1.85 ± 0.27	0.61 ± 0.24	0.77 ± 0.29
intestine	1.38 ± 0.38	7.38 ± 2.75	11.62 ± 3.42	7.68 ± 2.53	17.65 ± 2.91
thyroid	11.56 ± 2.61	14.93 ± 1.09	26.77 ± 1.41	23.53 ± 6.25	32.22 ± 1.13
		[^{125}I]**71** (Log D = 3.55 ± 0.02)			
blood	7.48 ± 0.81	6.02 ± 1.80	4.84 ± 1.40	3.35 ± 0.90	4.46 ± 0.92
brain	4.68 ± 0.25	2.62 ± 0.22	1.38 ± 0.23	0.71 ± 0.06	0.54 ± 0.09
heart	8.11 ± 1.74	4.14 ± 1.36	3.29 ± 1.42	1.74 ± 0.73	1.91 ± 0.60
liver	39.22 ± 4.48	40.83 ± 4.21	23.88 ± 4.99	22.63 ± 3.73	27.83 ± 2.15
spleen	4.57 ± 0.55	3.36 ± 0.14	2.22 ± 0.94	1.52 ± 0.38	1.23 ± 0.23
lung	9.67 ± 1.12	7.42 ± 2.95	6.18 ± 2.58	3.50 ± 0.70	3.90 ± 0.73
kidney	14.73 ± 2.23	16.49 ± 3.52	15.54 ± 5.56	10.46 ± 2.92	13.43 ± 4.53
stomach[a]	3.26 ± 1.37	3.82 ± 0.67	3.17 ± 0.97	3.34 ± 0.93	4.49 ± 0.82
intestine	3.53 ± 1.19	10.33 ± 4.30	13.19 ± 5.85	23.62 ± 3.87	41.29 ± 9.04
thyroid	18.20 ± 2.65	28.09 ± 4.45	27.78 ± 10.74	23.96 ± 3.78	72.93 ± 10.03
		[^{125}I]**70** (Log D = 3.26 ± 0.05)			
blood	3.89 ± 0.34	4.93 ± 1.91	4.12 ± 0.33	1.72 ± 0.58	2.52 ± 0.19
brain	4.56 ± 0.42	2.37 ± 0.32	1.36 ± 0.19	0.54 ± 0.12	0.40 ± 0.07
heart	7.06 ± 1.37	3.45 ± 0.59	2.01 ± 0.30	0.83 ± 0.17	1.11 ± 0.09
liver	16.98 ± 2.29	29.08 ± 4.93	24.17 ± 4.15	16.43 ± 2.32	17.57 ± 1.63
spleen	2.80 ± 0.15	2.02 ± 0.41	1.79 ± 0.17	0.80 ± 0.14	1.13 ± 0.39
lung	9.25 ± 1.09	6.06 ± 1.18	4.81 ± 0.43	2.43 ± 0.76	2.82 ± 0.16
kidney	11.20 ± 0.10	22.81 ± 3.42	16.31 ± 1.81	9.00 ± 1.67	9.52 ± 0.79
stomach[a]	1.37 ± 0.37	3.10 ± 2.24	3.12 ± 0.92	2.12 ± 0.62	3.07 ± 0.58
intestine	2.27 ± 0.17	6.90 ± 2.44	10.85 ± 3.68	25.97 ± 4.93	25.70 ± 1.48
thyroid	8.64 ± 2.19	8.39 ± 0.51	11.49 ± 3.53	14.14 ± 4.83	21.98 ± 3.75

[a] Expressed as % injected dose per organ.

(meta position)], which is consistent with previous data on primary, secondary, and tertiary amino ligands.[12,36] In contrast, methylation of the amino group at the ortho position reduced the binding affinity dramatically [e.g., **31** (K_i = 2636.5 ± 140.8 nM) ≫ **30** (K_i = 8.4 ± 3.0 nM)], which we will discuss later.

Increasing the size of the substituent at the para position does not affect the affinity for Aβ aggregates. The ligands **18** and **40** with a benzyloxy group showed K_i values of 2.0 ± 0.2 and 4.1 ± 0.4 nM, respectively, and **44** with a bulky trityloxy group also showed high affinity (K_i = 2.8 ± 0.4 nM). These results show high tolerance for steric bulk at this position. For the purpose of developing PET or SPECT agents targeting Aβ plaques, this finding regarding the dibenzylideneacetone scaffold is important. For example, a large chelating structure is necessary for technetium-99 m, and a long polyethylene glycol chain is adapted in the design of fluorine-18.[18,37,38] Indeed, the FPEG ligands **81**−**83** and **85** with different numbers of polyethylene glycol units (n = 1−3) all show excellent affinity (K_i < 10 nM), and the length of the linkage did not bring about an appreciable change in the binding properties. Interestingly, increasing the size of the substutient at the aromatic amino group decreased the binding affinity, as reflected in **16** with a *N*,*N*-diethylamino group (K_i = 15.7 ± 3.9 nM) and **17** with a *N*,*N*-diphenylamino group (K_i = 131.2 ± 20.3 nM).

The ligands with both electron-withdrawing substituents [e.g., F (**3** and **19**), NO_2 (**9** and **22**), and CF_3 (**14**)] and electron-donating substituents [e.g., OCH_3 (**8**) and $N(CH_3)_2$ (**12** and **25**)] at the para or meta position showed high affinity for Aβ aggregates, except for **13** with a carboxyl group (K_i = 78.1 ± 8.5 nM). Tolerance for steric bulk at the meta position was also observed, as the binding was not affected when different substituents were introduced [e.g., 3,5-$(CF_3)_2$ (**34**), 3,5-$(OCH_3)_2$ (**36**), and 3-phenoxy (**42**)]. In comparison, ligands with substituents at the ortho position showed less affinity for Aβ aggregates (K_i > 8 nM, e.g., **26**, **28**−**33**, **39**, **41**, and **43**) except for **27**. This may be due to the steric effects that arise between the ortho subsituents and the hydrogen atom on the carbon−carbon double bond, and the coplanar geometry of the conjugation π

dx.doi.org/10.1021/jm101404k |J. Med. Chem. 2011, 54, 2225–2240

system may be disrupted. As compared with **30**, the analogue with a *N*-methylamino group at the ortho position (**31**) exhibited greater steric effects, resulting in a loss of affinity.

When a phenyl ring in the dibenzylideneacetone structure is changed to a heterocyclic ring, such as a thiophene, furan, pyridine, or pyrrole ring, the ligands also show high affinity, as reflected in **44**−**55**. Use of a naphthalenyl group instead of the phenyl group (**56**) had little effect on binding affinity, consistent with the proposed $\pi-\pi$ interaction between ligands and Aβ fibers. There are distinct binding sites for CR and ThT on Aβ aggregates, which were clearly differentiated by Kung et al.[39] These two ligands did not inhibit each other, indicating that the two sites on Aβ aggregates are nonoverlapping.

A previous study using [^{125}I]IMSB as the radioligand showed that curcumin derivatives bound to Aβ aggregates at the CR site (curcumin, $K_i = 0.20 \pm 0.06$ nM; fluoropropyl-curcumin, $K_i = 0.07 \pm 0.01$).[32] However, in the present study, most of the dibenzylideneacetone ligands inhibited the binding of [^{125}I]IMPY to Aβ_{1-42} aggregates, indicating that they attach at the ThT-binding site. We consider the distance between the two phenyl rings important to the selection of the binding site. After removal of the active methylene moiety and one carbonyl moiety in the middle of curcumin, the distance between the two phenyl rings decreases, resulting in a change of the binding site.

Biological Evaluation. As compared with the binding of IMPY to Aβ_{1-42} aggregates (K_i = 10.5 nM), the affinity of iodinated compounds (**71**, **70**, and **6**) with primary, secondary, and tertiary amine groups and FPEG compounds (**83** and **85**, $n = 3$) was superior, and these compounds were evaluated further. The binding of these radiolabeled tracers to Aβ plaques in sections of brain tissue from AD patients or transgenic (Tg) model mice (APP/PS1) was evaluated by in vitro autoradiography. As shown in Figure 3A,C, two of the radioiodinated probes (**6** and **71**) exhibited intensive labeling of plaques showing a strong signal in the cortex region and a low background level in white matter in the AD brain sections. The hot spots of radioactivity were consistent with the results of immunohistochemical staining in vitro in the same sections using the Aβ antibody BC05 (Figure 3B,D). Autoradiographic studies of the two ^{18}F FPEG probes (**83** and **85**) were first performed with sections from Tg mice. Both ligands showed effective labeling of plaques and minimal background labeling (Figure 4A,E). The control cases were clearly void of any notable Aβ labeling (Figure 4B,F). The same sections were also stained with thioflavin-S, and the distribution of Aβ plaques perfectly accorded with the results of autoradiography (Figure 4C,G, red arrows). Autoradiographic studies of [^{18}F]**83** and [^{18}F]**85** were then performed with AD brain sections. As shown in Figure 5A,E, specific labeling of plaques was observed. Immunohistochemical staining confirmed the prescence of plaques in the sections (Figure 5B,D,G).

The lipophilicity (log *D*) of the radiolabeled tracers ([^{125}I]**6**, [^{125}I]**70**, [^{125}I]**71**, [^{18}F]**83**, and [^{18}F]**85**) measured under experimental conditions showed relatively high partition coefficients (log $D = 2.97-3.66$), a reflection of the lipophilic properties of these probes. Biodistribution experiments were performed in normal mice with these radiolabeled tracers. As shown in Tables 2 and 3, [^{125}I]**70** [^{125}I]**71**, [^{18}F]**83**, and [^{18}F]**85**, but not [^{125}I]**6**, exhibited good initial penetration of the BBB with excellent initial uptake in the brain (4.56, 4.68, 4.13, and 5.15% ID/g at 2 min, respectively). As compared with a previously reported radiofluorinated curcumin (0.52% ID/g at 2 min), these dibenzylideneacetones showed greatly improved uptake into the brain, suggesting them to have more suitable pharmacokinetic properties for imaging Aβ in AD brains. Because there are no plaques to cause the retention of Aβ-specific probes, the high uptake was subsequently followed by a fast washout (0.54, 0.71, 0.90, and 1.27% ID/g at 60 min). The tracer [^{125}I]**6** with a *N*, *N*-dimethylamino group showed a lower uptake at 2 min (1.59% ID/g), indicating low penetration of the intact BBB. Relatively high lipophilicity was observed for [^{125}I]**6** (log $D = 3.66 \pm 0.09$), and this disparity may account for the lower brain uptake and high blood uptake. The ratio $\text{brain}_{2\text{ min}}/\text{brain}_{60\text{ min}}$ is considered an important index with which to select tracers with appropriate kinetics in vivo. The five radiolabeled dibenzylideneacetone probes showed $\text{brain}_{2\text{ min}}/\text{brain}_{60\text{ min}}$ ratios of 5.68, 8.44, 6.59, 4.59, and 4.06 for [^{125}I]**6**, [^{125}I]**70**, [^{125}I]**71**, [^{18}F]**83**, and [^{18}F]**85**, respectively. As compared with [^{18}F]AV-45 (3.90), the two ^{18}F FPEG probes [^{18}F]**83** and [^{18}F]**85** had superior $\text{brain}_{2\text{ min}}/\text{brain}_{60\text{ min}}$ ratios. Accordingly, they may have better signal-to-noise ratios and therefore may be better for detecting Aβ plaques. Additionally, the thyroid uptake of the three radioiodinated probes ([^{125}I]**6**, [^{125}I]**70**, and [^{125}I]**71**) reached 14−24% ID/g at 1 h postinjection, which indicated deiodination in vivo. The defluorination, as reflected by bone uptake, for the two radiofluorinated probes ([^{18}F]**83** and [^{18}F]**85**) was low (2.33 and 2.54% ID/g at 1 h). As can be expected from the relatively high log *D* values, these radiolabeled tracers were cleared from plasma predominantly by the hepatobiliary system (ranging from 14.1 to 24.6% ID/g in liver and at 30 min pi). The hepatobiliar excretion to the intestines was also rather fast, and radioactivity was observed to accumulate within the intestine at later time points (ranging from 17.6 to 26.3% ID/g at 60 min pi). Also, a moderate uptake of these tracers was observed in the

Table 3. Biodistribution of [^{18}F]83 and [^{18}F]85 in ddY Normal Mice (% ID/g, Mean ± SD, $n = 4$)

organ	2 min	15 min	30 min	60 min
	[^{18}F]**83** (Log $D = 2.97 \pm 0.12$)			
brain	4.13 ± 0.41	1.51 ± 0.17	1.04 ± 0.23	0.90 ± 0.14
blood	5.38 ± 0.32	3.89 ± 0.36	2.46 ± 0.54	1.60 ± 0.17
bone	2.88 ± 0.37	2.42 ± 0.14	2.08 ± 0.54	2.33 ± 0.30
liver	22.32 ± 3.12	24.41 ± 3.34	14.07 ± 1.94	6.88 ± 1.51
kidney	12.95 ± 0.79	12.77 ± 2.42	7.13 ± 2.64	3.67 ± 0.85
spleen	4.26 ± 1.05	6.19 ± 1.06	4.46 ± 0.80	1.93 ± 0.67
stomach[a]	6.28 ± 5.75	7.39 ± 1.87	6.00 ± 1.14	3.98 ± 1.52
intestine	4.12 ± 0.48	10.53 ± 2.11	17.50 ± 4.47	21.57 ± 7.37
lung	12.30 ± 1.99	6.34 ± 0.88	3.38 ± 0.43	1.86 ± 0.25
heart	7.60 ± 1.32	3.33 ± 0.35	1.90 ± 0.26	1.47 ± 0.13
	[^{18}F]**85** (Log $D = 3.08 \pm 0.05$)			
brain	5.15 ± 0.17	1.89 ± 0.17	1.35 ± 0.19	1.27 ± 0.12
blood	7.44 ± 1.22	7.99 ± 0.34	4.68 ± 0.59	3.59 ± 0.93
bone	2.97 ± 0.35	2.93 ± 0.37	2.94 ± 0.91	2.54 ± 0.84
liver	24.15 ± 5.77	30.09 ± 4.43	19.24 ± 3.64	14.07 ± 1.87
kidney	16.48 ± 2.51	14.15 ± 0.98	11.51 ± 1.76	9.43 ± 1.50
spleen	5.39 ± 1.79	6.62 ± 0.42	5.44 ± 1.24	5.35 ± 2.06
stomach[a]	3.26 ± 0.63	2.61 ± 0.18	1.93 ± 0.33	1.28 ± 0.49
intestine	6.58 ± 0.89	12.82 ± 3.23	24.34 ± 3.83	26.26 ± 3.57
lung	12.19 ± 2.31	11.77 ± 1.94	7.43 ± 1.03	5.44 ± 1.45
heart	10.55 ± 1.10	7.64 ± 1.23	5.67 ± 0.72	5.14 ± 0.88

[a] Expressed as % injected dose per organ.

dx.doi.org/10.1021/jm101404k |*J. Med. Chem.* 2011, 54, 2225–2240

kidneys, indicating that they too were excreted via the renal system.

■ CONCLUSIONS

In conclusion, a new series of novel dibenzylideneacetone derivatives, containing various substituents, were successfully prepared as a new backbone structure for Aβ imaging agents. Most of them displayed excellent affinity for Aβ aggregates (K_i in the nM range). The SAR study described above indicated that the introduction of a substituted group at the ortho position reduced or abolished the binding. However, the para position was highly tolerant of steric bulk substitutions, which opens up the possibility of developing new, easily labeled radioligands for imaging Aβ plaques in vivo. Furthermore, the radiolabeled probes showed good penetration and fast washout in the mouse brain. A specific plaque-labeling signal was clearly demonstrated for these probes in Tg mouse brain sections as well as postmortem AD brain sections. Taken together, the present results suggest that these novel dibenzylideneacetones may be useful probes for the diagnosis of AD. Additional chemical modifications of the dibenzylideneacetone structure may lead to more useful Aβ imaging agents for both PET and SPECT.

■ EXPERIMENTAL SECTION

All of the chemicals used were commercial products employed without further purification. The ^{1}H NMR spectra were obtained at 400 MHz on Jeol JNM-AL400 NMR spectrometers in $CDCl_3$ solutions at room temperature with TMS as an internal standard. Chemical shifts are reported as δ values relative to the internal TMS. Coupling constants are reported in Hertz. Multiplicity is defined by s (singlet), d (doublet), t (triplet), and m (multiplet). Mass spectra were acquired with a Shimadzu GC-MS-QP2010 Plus (ESI). HPLC was performed with a Shimadzu system (a LC-20AT pump with a SPD-20A UV detector, λ = 254 nm) using a column of Cosmosil C18 (Nakalai Tesque, $5C_{18}$-AR-II, 4.6 mm × 150 mm or 10 mm × 150 mm) and acetonitrile/water as the mobile phase. Fluorescence was observed with a Nikon Eclipse 80i microscope equipped with a BV-2A filter set (excitation, 400−440 nm; diachronic mirror, 455 nm; and long pass filter, 470 nm). The purity of the synthesized compounds was determined using analytical HPLC and was found to be more than 95%.

Chemistry. *General Procedure A: Preparation of Compounds **2**−**9**, **12**−**22**, **26**−**29**, and **32**−**48**.* To a solution of **1** (1−2 mmol) and substitued aromatic aldehydes (1−2 mmol) in 20 mL of ethanol was added 0.2 mL of NaOMe (28% in methanol). The reaction mixture was stirred for 12 h at room temperature. The precipitate was collected by filtration, washed with water and hexane, and recrystallized from ethanol or purified by silica gel chromatography to afford the final products.

*General Procedure B: Preparation of Compounds **10**, **23**, and **30**.* A mixture of nitro compounds (1−2 mmol) and $SnCl_2$ (2−4 mmol) dissolved in 20 mL of ethanol containing 4 mL of concentrated hydrochloric acid was stirred under reflux for 2 h. After the mixture had cooled to room temperature, 2 M NaOH (50 mL) was added and extracted with ethyl acetate (100 mL). The organic layer was dried over Na_2SO_4. The solvent was removed, and the residue was purified by silica gel chromatography to afford the final products.

*General Procedure C: Preparation of Compounds **11**, **24**, **25**, and **31**.* To a solution of amino compounds (1−2 mmol) and K_2CO_3 (1−2 mmol) in 20 mL of acetone was added CH_3I (2−4 mmol) dropwise, and the reaction mixture was stirred for 8 h at room temperature. After evaporation, the solvent was removed, and the residue was purified by silica gel chromatography to afford the final products.

*(E)-4-(4-(Dimethylamino)phenyl)but-3-en-2-one (**1**).* To a solution of 4-(dimethylamino)benzaldehyde (14.92 g, 100 mmol) in 300 mL of acetone was added 10 mL of NaOH (1 M), and the reaction mixture was stirred for 12 h at room temperature. The solvent was concentrated to 100 mL, 300 mL of water was added, and the yellow crystal that formed was collected by filtration, washed with water and cold hexane, and then dried under vacuum to obtain 13.70 g of **1** (72.5%). ^{1}H NMR (400 MHz, $CDCL_3$): δ 7.46 (d, J = 16.1 Hz, 1H), 7.44 (d, J = 9.0 Hz, 2H), 6.68 (d, J = 8.9 Hz, 2H), 6.55 (d, J = 16.1 Hz, 1H), 3.03 (s, 6H), 2.34 (s, 3H). MS (ESI): m/z calcd for $C_{12}H_{15}NO$, 189.12; found, 190.10 ($M + H^+$).

*(1E,4E)-1-(4-(Dimethylamino)phenyl)-5-phenylpenta-1,4-dien-3-one (**2**).* Compound **2** was prepared following general procedure A. Yield, 31.6%. ^{1}H NMR (400 MHz, $CDCL_3$): δ 7.73 (d, J = 15.8 Hz, 1H), 7.71 (d, J = 15.9 Hz, 1H), 7.62 (dd, J = 7.5, 2.0 Hz, 2H), 7.53 (d, J = 8.9 Hz, 2H), 7.45−7.33 (m, 3H), 7.10 (d, J = 15.9 Hz, 1H), 6.89 (d, J = 15.8 Hz, 1H), 6.70 (d, J = 8.9 Hz, 2H), 3.05 (s, 6H). MS (ESI): m/z calcd for $C_{19}H_{19}NO$ 277.15; found 278.15 ($M + H^+$).

*(1E,4E)-1-(4-(Dimethylamino)phenyl)-5-(4-fluorophenyl)penta-1,4-dien-3-one (**3**).* Compound **3** was prepared following general procedure A. Yield, 77.3%. ^{1}H NMR (400 MHz, $CDCL_3$): δ 7.74 (d, J = 15.8 Hz, 1H), 7.69 (d, J = 15.9 Hz, 1H), 7.62 (dd, J = 8.7, 5.4 Hz, 2H), 7.54 (d, J = 8.9 Hz, 2H), 7.11 (t, J = 8.6 Hz, 2H), 7.04 (d, J = 15.9 Hz, 1H), 6.88 (d, J = 15.7 Hz, 1H), 6.72 (d, J = 8.9 Hz, 2H), 3.06 (s, 6H). MS (ESI): m/z calcd for $C_{19}H_{18}FNO$ 295.14; found 296.15 ($M + H^+$).

*(1E,4E)-1-(4-Chlorophenyl)-5-(4-(dimethylamino)phenyl)penta-1,4-dien-3-one (**4**).* Compound **4** was prepared following general procedure A. Yield, 78.5%. ^{1}H NMR (400 MHz, $CDCL_3$): δ 7.72 (d, J = 15.7 Hz, 1H), 7.65 (d, J = 15.9 Hz, 1H), 7.54 (d, J = 8.2 Hz, 2H), 7.52 (d, J = 8.6 Hz, 2H), 7.37 (d, J = 8.5 Hz, 2H), 7.06 (d, J = 15.9 Hz, 1H), 6.85 (d, J = 15.8 Hz, 1H), 6.69 (d, J = 8.9 Hz, 2H), 3.05 (s, 6H). MS (ESI): m/z calcd for $C_{19}H_{18}ClNO$, 311.11; found, 312.10 ($M + H^+$).

*(1E,4E)-1-(4-Bromophenyl)-5-(4-(dimethylamino)phenyl)penta-1,4-dien-3-one (**5**).* Compound **5** was prepared following general procedure A. Yield, 49.4%. ^{1}H NMR (400 MHz, $CDCL_3$): δ 7.72 (d, J = 15.7 Hz, 1H), 7.63 (d, J = 15.9 Hz, 1H), 7.55−7.50 (m, 4H), 7.47 (d, J = 8.5 Hz, 2H), 7.08 (d, J = 15.8 Hz, 1H), 6.86 (d, J = 15.7 Hz, 1H), 6.70 (d, J = 8.8 Hz, 2H), 3.05 (s, 6H). MS (ESI): m/z calcd for $C_{19}H_{18}BrNO$, 355.06; found, 356.05 ($M + H^+$).

*(1E,4E)-1-(4-(Dimethylamino)phenyl)-5-(4-iodophenyl)penta-1,4-dien-3-one (**6**).* Compound **6** was prepared following general procedure A. Yield, 61.5%. ^{1}H NMR (400 MHz, $CDCL_3$): δ 7.76 (d, J = 8.4 Hz, 2H), 7.74 (d, J = 15.8 Hz, 1H), 7.63 (d, J = 15.8 Hz, 1H), 7.54 (d, J = 8.9 Hz, 2H), 7.35 (d, J = 8.5 Hz, 2H), 7.11 (d, J = 15.9 Hz, 1H), 6.88 (d, J = 15.7 Hz, 1H), 6.72 (d, J = 8.9 Hz, 2H), 3.07 (s, 6H). HRMS (EI): m/z (EI^+): calcd for $C_{19}H_{18}INO$, 403.0433; found, 403.0426 ($M + H^+$).

*(1E,4E)-1-(4-(Dimethylamino)phenyl)-5-(4-hydroxyphenyl)penta-1,4-dien-3-one (**7**).* Compound **7** was prepared following general procedure A. Yield, 19.5%. ^{1}H NMR (400 MHz, CD_3OD): δ 7.72 (d, J = 16.3 Hz, 1H), 7.67 (d, J = 16.4 Hz, 1H), 7.56 (d, J = 8.8 Hz, 4H), 7.05 (d, J = 15.8 Hz, 1H), 6.97 (d, J = 15.7 Hz, 1H), 6.83 (d, J = 8.6 Hz, 2H), 6.76 (d, J = 9.0 Hz, 2H), 3.03 (s, 6H). MS (ESI): m/z calcd for $C_{19}H_{19}NO_2$, 293.14; found, 294.20 ($M + H^+$).

*(1E,4E)-1-(4-(Dimethylamino)phenyl)-5-(4-methoxyphenyl)penta-1,4-dien-3-one (**8**).* Compound **8** was prepared following general procedure A. Yield, 71.3%. ^{1}H NMR (400 MHz, $CDCL_3$): δ 7.73 (d, J = 15.8 Hz, 1H), 7.70 (d, J = 15.8 Hz, 1H), 7.59 (d, J = 8.8 Hz, 2H), 7.53 (d, J = 8.9 Hz, 2H), 6.99 (d, J = 15.8 Hz, 1H), 6.95 (d, J = 8.8 Hz, 2H), 6.89 (d, J = 15.7 Hz, 1H), 6.71 (d, J = 8.9 Hz, 2H), 3.87 (s, 3H), 3.05 (s, 6H). MS (ESI): m/z calcd for $C_{20}H_{21}NO_2$, 307.16; found, 308.15 ($M + H^+$).

*(1E,4E)-1-(4-(Dimethylamino)phenyl)-5-(4-nitrophenyl)penta-1,4-dien-3-one (**9**).* Compound **9** was prepared following general procedure A. Yield, 64.3%. ^{1}H NMR (400 MHz, $CDCL_3$): δ 8.28 (d, J = 8.8 Hz, 2H), 7.77 (d, J = 14.9 Hz, 1H), 7.77 (d, J = 9.0 Hz, 2H), 7.73 (d, J = 15.2 Hz,

1H), 7.55 (d, J = 8.9 Hz, 2H), 7.22 (d, J = 15.8 Hz, 1H), 6.88 (d, J = 15.8 Hz, 1H), 6.72 (d, J = 8.9 Hz, 2H), 3.08 (s, 6H). MS (ESI): m/z calcd for $C_{19}H_{18}N_2O_3$, 322.13; found, 323.10 ($M + H^+$).

*(1E,4E)-1-(4-Aminophenyl)-5-(4-(dimethylamino)phenyl)penta-1,4-dien-3-one (**10**).* Compound **10** was prepared following general procedure B. Yield, 11.5%. ^{1}H NMR (400 MHz, $CDCl_3$): δ 7.71 (d, J = 15.1 Hz, 1H), 7.67 (d, J = 15.1 Hz, 1H), 7.53 (d, J = 8.8 Hz, 2H), 7.47 (d, J = 8.4 Hz, 2H), 6.93 (d, J = 15.8 Hz, 1H), 6.89 (d, J = 15.7 Hz, 1H), 6.72 (d, J = 8.5 Hz, 2H), 6.69 (d, J = 8.2 Hz, 2H), 3.98 (s, 2H), 3.06 (s, 6H). MS (ESI): m/z calcd for $C_{19}H_{20}N_2O$, 292.16; found, 293.15 ($M + H^+$).

*(1E,4E)-1-(4-(Dimethylamino)phenyl)-5-(4-(methylamino)phenyl)penta-1,4-dien-3-one (**11**).* Compound **11** was prepared following general procedure C. Yield, 6.2%. ^{1}H NMR (400 MHz, $CDCl_3$): δ 7.68 (d, J = 16.3 Hz, 1H), 7.67 (d, J = 15.7 Hz, 1H), 7.51 (d, J = 8.9 Hz, 2H), 7.48 (d, J = 8.6 Hz, 2H), 6.88 (d, J = 15.7 Hz, 1H), 6.88 (d, J = 15.7 Hz, 1H), 6.69 (d, J = 8.9 Hz, 2H), 6.59 (d, J = 8.6 Hz, 2H), 3.04 (s, 6H), 2.89 (s, 3H). MS (ESI): m/z calcd for $C_{20}H_{22}N_2O$, 306.176; found, 307.20 ($M + H^+$).

*(1E,4E)-1,5-Bis(4-(dimethylamino)phenyl)penta-1,4-dien-3-one (**12**).* Compound **12** was prepared following general procedure A. Yield, 32.2%. ^{1}H NMR (400 MHz, $CDCL_3$): δ 7.71 (d, J = 15.7 Hz, 2H), 7.54 (d, J = 8.9 Hz, 4H), 6.91 (d, J = 15.7 Hz, 2H), 6.72 (d, J = 8.9 Hz, 4H), 3.06 (s, 12H). MS (ESI): m/z calcd for $C_{21}H_{24}N_2O$, 320.19; found, 321.20 ($M + H^+$).

*4-((1E,4E)-5-(4-(Dimethylamino)phenyl)-3-oxopenta-1,4-dien-1-yl)-benzoic Acid (**13**).* Compound **13** was prepared following general procedure A. Yield, 2.5%. ^{1}H NMR (400 MHz, $CDCL_3$): δ 8.14 (d, J = 8.3 Hz, 2H), 7.75 (d, J = 15.8 Hz, 1H), 7.73 (d, J = 15.6 Hz, 1H), 7.71 (d, J = 8.1 Hz, 2H), 7.54 (d, J = 8.8 Hz, 2H), 7.20 (d, J = 15.9 Hz, 1H), 6.88 (d, J = 15.7 Hz, 1H), 6.71 (d, J = 8.8 Hz, 2H), 3.06 (s, 6H). MS (ESI): m/z calcd for $C_{20}H_{19}NO_3$, 321.14; found, 322.10 ($M + H^+$).

*(1E,4E)-1-(4-(Dimethylamino)phenyl)-5-(4-(trifluoromethyl)phenyl)penta-1,4-dien-3-one (**14**).* Compound **14** was prepared following general procedure A. Yield, 79.9%. ^{1}H NMR (400 MHz, $CDCL_3$): δ 7.76 (d, J = 15.9 Hz, 1H), 7.75–7.66 (m, 5H), 7.55 (d, J = 8.8 Hz, 2H), 7.17 (d, J = 15.9 Hz, 1H), 6.89 (d, J = 15.7 Hz, 1H), 6.72 (d, J = 8.9 Hz, 2H), 3.08 (s, 6H). MS (ESI): m/z calcd for $C_{20}H_{18}F_3NO$, 345.13; found, 346.15 ($M + H^+$).

*(1E,4E)-1-(4-(Dimethylamino)phenyl)-5-(p-tolyl)penta-1,4-dien-3-one (**15**).* Compound **15** was prepared following general procedure A. Yield, 84.5%. ^{1}H NMR (400 MHz, $CDCL_3$): δ 7.74 (d, J = 15.8 Hz, 1H), 7.72 (d, J = 15.9 Hz, 1H), 7.55 (d, J = 8.9 Hz, 2H), 7.54 (d, J = 8.0 Hz, 2H), 7.24 (d, J = 8.0 Hz, 2H), 7.08 (d, J = 15.9 Hz, 1H), 6.91 (d, J = 15.7 Hz, 1H), 6.72 (d, J = 8.9 Hz, 2H), 3.07 (s, 6H), 2.41 (s, 3H). MS (ESI): m/z calcd for $C_{21}H_{20}NO$, 291.16; found, 292.00 ($M + H^+$).

*(1E,4E)-1-(4-(Diethylamino)phenyl)-5-(4-(dimethylamino)phenyl)penta-1,4-dien-3-one (**16**).* Compound **16** was prepared following general procedure A. Yield, 46.2%. ^{1}H NMR (400 MHz, $CDCL_3$): δ 7.47 (d, J = 15.9 Hz, 2H), 7.44 (d, J = 8.9 Hz, 4H), 6.68 (d, J = 8.8 Hz, 4H), 6.55 (d, J = 16.1 Hz, 2H), 3.03 (s, 12H), 2.34 (s, 6H). MS (ESI): m/z calcd for $C_{23}H_{28}N_2O$, 348.22; found, 349.20 ($M + H^+$).

*(1E,4E)-1-(4-(Dimethylamino)phenyl)-5-(4-(diphenylamino)phenyl)penta-1,4-dien-3-one (**17**).* Compound **17** was prepared following general procedure A. Yield, 41.7%. ^{1}H NMR (400 MHz, $CDCL_3$): δ 7.70 (d, J = 15.4 Hz, 1H), 7.66 (d, J = 15.5 Hz, 1H), 7.52 (d, J = 8.8 Hz, 2H), 7.46 (d, J = 8.7 Hz, 2H), 7.30 (t, J = 7.9 Hz, 4H), 7.14 (dd, J = 7.7, 0.9 Hz, 4H), 7.09 (td, J = 7.5, 1.0 Hz, 2H), 7.02 (d, J = 8.6 Hz, 2H), 6.95 (d, J = 15.8 Hz, 1H), 6.87 (d, J = 15.7 Hz, 1H), 6.69 (d, J = 8.8 Hz, 2H), 3.04 (s, 6H). MS (ESI): m/z calcd for $C_{31}H_{28}N_2O$, 444.22; found, 445.15 ($M + H^+$).

*(1E,4E)-1-(4-(Benzyloxy)phenyl)-5-(4-(dimethylamino)phenyl)penta-1,4-dien-3-one (**18**).* Compound **18** was prepared following general procedure A. Yield, 27.4%. ^{1}H NMR (400 MHz, $CDCL_3$): δ 7.70 (d, J = 15.8 Hz, 1H), 7.68 (d, J = 15.7 Hz, 1H), 7.57 (d, J = 8.7 Hz, 2H), 7.52 (d, J = 8.9 Hz, 2H), 7.47–7.31 (m, 5H), 7.00 (d, J = 8.8 Hz, 2H), 6.97 (d, J = 15.7 Hz, 1H), 6.87 (d, J = 15.8 Hz, 1H), 6.70 (d, J = 8.9 Hz, 2H), 5.11 (s, 2H), 3.04 (s, 6H). MS (ESI): m/z calcd for $C_{26}H_{25}NO_2$, 383.19; found, 384.25 ($M + H^+$).

*(1E,4E)-1-(4-(Dimethylamino)phenyl)-5-(3-fluorophenyl)penta-1,4-dien-3-one (**19**).* Compound **19** was prepared following general procedure A. Yield, 63.4%. ^{1}H NMR (400 MHz, $CDCL_3$): δ 7.87 (d, J = 15.8 Hz, 1H), 7.79 (d, J = 15.8 Hz, 1H), 7.67 (d, J = 8.9 Hz, 2H), 7.51 (ddd, J = 5.4, 3.7, 1.7 Hz, 2H), 7.45 (dd, J = 10.2, 3.0 Hz, 1H), 7.22 (d, J = 15.8 Hz, 1H), 7.00 (d, J = 15.7 Hz, 1H), 6.84 (d, J = 8.9 Hz, 2H), 3.19 (s, 6H). MS (ESI): m/z calcd for $C_{19}H_{18}FNO$, 295.14; found, 296.10 ($M + H^+$).

*(1E,4E)-1-(3-Bromophenyl)-5-(4-(dimethylamino)phenyl)penta-1,4-dien-3-one (**20**).* Compound **20** was prepared following general procedure A. Yield, 77.5%. ^{1}H NMR (400 MHz, $CDCL_3$): δ 7.79 (t, J = 1.7 Hz, 1H), 7.75 (d, J = 15.8 Hz, 1H), 7.64 (d, J = 15.8 Hz, 1H), 7.58–7.50 (m, 4H), 7.30 (t, J = 7.9 Hz, 1H), 7.11 (d, J = 15.8 Hz, 1H), 6.88 (d, J = 15.7 Hz, 1H), 6.72 (d, J = 8.9 Hz, 2H), 3.08 (s, 6H). MS (ESI): m/z calcd for $C_{19}H_{18}BrNO$, 355.06; found, 356.05 ($M + H^+$).

*(1E,4E)-1-(4-(Dimethylamino)phenyl)-5-(3-iodophenyl)penta-1,4-dien-3-one (**21**).* Compound **21** was prepared following general procedure A. Yield, 57.3%. ^{1}H NMR (400 MHz, $CDCL_3$): δ 7.98(s, 1H), 7.73 (d, J = 15.6 Hz, 1H), 7.71 (d, J = 7.6 Hz, 1H), 7.61–7.52 (m, 4H), 7.15 (t, J = 7.6 Hz, 1H), 7.08 (d, J = 16.0 Hz, 1H), 6.86 (d, J = 15.6 Hz, 1H), 6.71 (d, J = 9.2 Hz, 2H), 3.06 (s, 6H). MS (ESI): m/z calcd for $C_{19}H_{18}INO$, 403.04; found, 404.05 ($M + H^+$).

*(1E,4E)-1-(4-(Dimethylamino)phenyl)-5-(3-nitrophenyl)penta-1,4-dien-3-one (**22**).* Compound **22** was prepared following general procedure A. Yield, 39.4%. ^{1}H NMR (400 MHz, $CDCL_3$): δ 8.49 (s, 1H), 8.23 (dd, J = 8.2, 2.2 Hz, 1H), 7.88 (d, J = 7.8 Hz, 1H), 7.76 (d, J = 15.2 Hz, 1H), 7.72 (d, J = 14.8 Hz, 1H), 7.59 (t, J = 8.0 Hz, 1H), 7.54 (d, J = 8.6 Hz, 2H), 7.22 (d, J = 15.9 Hz, 1H), 6.87 (d, J = 15.8 Hz, 1H), 6.71 (d, J = 8.8 Hz, 2H), 3.06 (s, 6H). MS (ESI): m/z calcd for $C_{19}H_{18}N_2O_3$, 322.13; found, 323.15 ($M + H^+$).

*(1E,4E)-1-(3-Aminophenyl)-5-(4-(dimethylamino)phenyl)penta-1,4-dien-3-one (**23**).* Compound **23** was prepared following general procedure B. Yield, 40.9%. ^{1}H NMR (400 MHz, $CDCL_3$): δ 7.71 (d, J = 15.7 Hz, 1H), 7.62 (d, J = 15.9 Hz, 1H), 7.52 (d, J = 8.9 Hz, 2H), 7.19 (t, J = 7.8 Hz, 1H), 7.04 (d, J = 2.3 Hz, 1H), 7.03 (d, J = 15.9 Hz, 1H), 6.92 (d, J = 1.8 Hz, 1H), 6.87 (d, J = 15.7 Hz, 1H), 6.71 (dd, J = 9.9, 2.3 Hz, 1H), 6.70 (d, J = 8.9 Hz, 2H), 3.74 (s, 2H), 3.05 (s, 6H). MS (ESI): m/z calcd for $C_{19}H_{20}N_2O$, 292.16; found, 293.10 ($M + H^+$).

*(1E,4E)-1-(4-(Dimethylamino)phenyl)-5-(3-(methylamino)phenyl)penta-1,4-dien-3-one (**24**).* Compound **24** was prepared following general procedure C. Yield, 30.0%. ^{1}H NMR (400 MHz, $CDCL_3$): δ 7.73 (d, J = 15.7 Hz, 1H), 7.67 (d, J = 15.8 Hz, 1H), 7.54 (d, J = 8.9 Hz, 2H), 7.24 (t, J = 7.8 Hz, 1H), 7.06 (d, J = 15.9 Hz, 1H), 7.01 (d, J = 7.6 Hz, 1H), 6.92 (d, J = 15.8 Hz, 1H), 6.84 (s, 1H), 6.72 (d, J = 8.9 Hz, 2H), 6.67 (d, J = 8.0 Hz, 1H), 3.07 (s, 6H), 2.90 (s, 3H). MS (ESI): m/z calcd for $C_{20}H_{22}N_2O$, 306.17; found, 307.15 ($M + H^+$).

*(1E,4E)-1-(3-(Dimethylamino)phenyl)-5-(4-(dimethylamino)phenyl)penta-1,4-dien-3-one (**25**).* Compound **25** was prepared following general procedure C. Yield, 28.4%. ^{1}H NMR (400 MHz, $CDCL_3$): δ 7.72 (d, J = 15.7 Hz, 1H), 7.68 (d, J = 15.8 Hz, 1H), 7.53 (d, J = 8.7 Hz, 2H), 7.27 (t, J = 7.7 Hz, 1H), 7.05 (dd, J = 15.9, 0.7 Hz, 1H), 7.01 (d, J = 7.3 Hz, 1H), 6.93 (s, 1H), 6.91 (dd, J = 15.7, 0.8 Hz, 1H), 6.78 (dd, J = 8.1, 2.4 Hz, 1H), 6.70 (d, J = 8.6 Hz, 2H), 3.04 (s, 6H), 2.99 (s, 6H). MS (ESI): m/z calcd for $C_{21}H_{24}N_2O$, 320.19; found, 321.10 ($M + H^+$).

*(1E,4E)-1-(2-(Benzyloxy)phenyl)-5-(4-(dimethylamino)phenyl)penta-1,4-dien-3-one (**26**).* Compound **26** was prepared following general procedure A. Yield, 51.0%. ^{1}H NMR (400 MHz, $CDCL_3$): δ 8.06 (d, J = 16.1 Hz, 1H), 7.62 (d, J = 7.4 Hz, 1H), 7.61 (d, J = 15.8 Hz, 2H), 7.53–7.28 (m, 10H), 7.23 (d, J = 16.1 Hz, 1H), 7.00 (t, J = 8.1 Hz, 2H), 6.85 (d, J = 15.8 Hz, 1H), 6.68 (d, J = 8.8 Hz, 2H), 5.19 (s, 2H), 3.04 (s, 8H). MS (ESI): m/z calcd for $C_{26}H_{25}NO_2$, 383.19; found, 384.15 ($M + H^+$).

(1E,4E)-1-(2-Chlorophenyl)-5-(4-(dimethylamino)phenyl)penta-1,4-dien-3-one (**27**). Compound **27** was prepared following general procedure A. Yield, 78.5%. ^{1}H NMR (400 MHz, $CDCL_3$): δ 7.72 (d, J = 15.7 Hz, 1H), 7.62 (d, J = 16.0 Hz, 2H), 7.60 (s, 1H), 7.52 (d, J = 8.9 Hz, 2H), 7.48−7.45 (m, 1H), 7.39−7.32 (m, 2H), 7.09 (d, J = 15.8 Hz, 1H), 6.85 (d, J = 15.8 Hz, 1H), 6.70 (d, J = 8.9 Hz, 2H), 3.05 (s, 6H). MS (ESI): m/z calcd for $C_{19}H_{18}ClNO$, 311.11; found, 312.15 ($M + H^+$).

(1E,4E)-1-(4-(Dimethylamino)phenyl)-5-(2-hydroxyphenyl)penta-1,4-dien-3-one (**28**). Compound **28** was prepared following general procedure A. Yield, 37.2%. ^{1}H NMR (400 MHz, $CDCL_3$): δ 8.09 (d, J = 16.1 Hz, 1H), 7.76 (d, J = 15.7 Hz, 1H), 7.59 (d, J = 7.6 Hz, 1H), 7.55 (d, J = 8.8 Hz, 2H), 7.33−7.21 (m, 2H), 7.00−6.90 (m, 3H), 6.71 (d, J = 8.8 Hz, 2H), 3.06 (s, 6H). MS (ESI): m/z calcd for $C_{19}H_{19}NO_2$, 293.14; found, 294.00 ($M + H^+$).

(1E,4E)-1-(4-(Dimethylamino)phenyl)-5-(2-nitrophenyl)penta-1,4-dien-3-one (**29**). Compound **29** was prepared following general procedure A. Yield, 35.8%. ^{1}H NMR (400 MHz, $CDCL_3$): δ 8.07 (d, J = 15.9 Hz, 1H), 8.05 (dd, J = 8.1, 1.2 Hz, 1H), 7.75 (d, J = 15.8 Hz, 1H), 7.73 (dd, J = 7.7, 1.5 Hz, 1H), 7.66 (td, J = 7.8, 1.3 Hz, 1H), 7.55 (d, J = 7.7 Hz, 1H), 7.53 (d, J = 8.9 Hz, 2H), 6.93 (d, J = 15.9 Hz, 1H), 6.92 (d, J = 15.7 Hz, 1H), 6.70 (d, J = 8.9 Hz, 2H), 3.05 (s, 6H). MS (ESI): m/z calcd for $C_{19}H_{18}N_2O_3$, 322.13; found, 323.15 ($M + H^+$).

(1E,4E)-1-(2-Aminophenyl)-5-(4-(dimethylamino)phenyl)penta-1,4-dien-3-one (**30**). Compound **30** was prepared following general procedure B. Yield, 41.4%. ^{1}H NMR (400 MHz, $CDCL_3$): δ 8.09 (d, J = 15.4 Hz, 1H), 8.07 (d, J = 15.6 Hz, 1H), 7.78 (d, J = 8.1 Hz, 1H), 7.70 (ddd, J = 8.4, 6.9, 1.5 Hz, 1H), 7.67 (d, J = 8.6 Hz, 1H), 7.64 (d, J = 16.3 Hz, 1H), 7.57 (d, J = 8.9 Hz, 2H), 7.48 (ddd, J = 8.0, 6.9, 1.1 Hz, 1H), 7.25 (d, J = 16.3 Hz, 1H), 6.76 (d, J = 8.9 Hz, 2H), 3.04 (s, 6H). MS (ESI): m/z calcd for $C_{19}H_{20}N_2O$, 292.16; found, 293.00 ($M + H^+$).

(1E,4E)-1-(4-(Dimethylamino)phenyl)-5-(2-(methylamino)phenyl)penta-1,4-dien-3-one (**31**). Compound **31** was prepared following general procedure C. Yield, 82.4%. ^{1}H NMR (400 MHz, $CDCL_3$): δ 8.35 (d, J = 8.8 Hz, 1H), 8.03 (d, J = 8.4 Hz, 1H), 8.00−7.92 (m, 6H), 7.84 (d, J = 16.2 Hz, 1H), 7.78 (t, J = 7.2 Hz, 1H), 7.59 (d, J = 16.2 Hz, 1H), 7.56 (d, J = 16.4 Hz, 1H), 3.72 (s, 9H). MS (ESI): m/z calcd for $C_{20}H_{22}N_2O$, 306.17; found, 307.10 ($M + H^+$).

(1E,4E)-1-(2,6-Dichlorophenyl)-5-(4-(dimethylamino)phenyl)penta-1,4-dien-3-one (**32**). Compound **32** was prepared following general procedure A. Yield, 6.3%. ^{1}H NMR (400 MHz, $CDCL_3$): δ 7.77 (d, J = 16.2 Hz, 1H), 7.74 (d, J = 15.8 Hz, 1H), 7.54 (d, J = 8.9 Hz, 2H), 7.40 (d, J = 8.1 Hz, 2H), 7.25 (d, J = 16.2 Hz, 1H), 7.21 (t, J = 8.0 Hz, 1H), 6.88 (d, J = 15.8 Hz, 1H), 6.72 (d, J = 8.9 Hz, 2H), 3.07 (s, 6H). MS (ESI): m/z calcd for $C_{19}H_{17}Cl_2NO$, 345.07; found, 346.95 ($M + H^+$).

(1E,4E)-1-(2-Chloro-6-fluorophenyl)-5-(4-(dimethylamino)phenyl)penta-1,4-dien-3-one (**33**). Compound **33** was prepared following general procedure A. Yield, 62.5%. ^{1}H NMR (400 MHz, $CDCL_3$): δ 7.91 (d, J = 16.2 Hz, 1H), 7.75 (d, J = 15.8 Hz, 1H), 7.55 (d, J = 8.9 Hz, 2H), 7.39 (d, J = 16.2 Hz, 1H), 7.35−7.22 (m, 2H), 7.16−7.02 (m, 1H), 6.88 (d, J = 15.8 Hz, 1H), 6.72 (d, J = 8.9 Hz, 2H), 3.07 (s, 6H). MS (ESI): m/z calcd for $C_{19}H_{17}ClFNO$, 329.10; found, 330.15 ($M + H^+$).

(1E,4E)-1-(3,5-Bis(trifluoromethyl)phenyl)-5-(4-(dimethylamino)phenyl)penta-1,4-dien-3-one (**34**). Compound **34** was prepared following general procedure A. Yield, 21.3%. ^{1}H NMR (400 MHz, $CDCL_3$): δ 8.01 (s, 1H), 7.87 (s, 1H), 7.76 (d, J = 15.8 Hz, 1H), 7.72 (d, J = 15.9 Hz, 1H), 7.54 (d, J = 8.9 Hz, 1H), 7.21 (d, J = 15.8 Hz, 1H), 6.86 (d, J = 15.7 Hz, 1H), 6.70 (d, J = 8.9 Hz, 1H), 3.06 (s, 6H). MS (ESI): m/z calcd for $C_{21}H_{17}F_6NO$, 413.12; found, 413.85 ($M + H^+$).

(1E,4E)-1-(3,4-Dimethoxyphenyl)-5-(4-(dimethylamino)phenyl)penta-1,4-dien-3-one (**35**). Compound **35** was prepared following general procedure A. Yield, 40.8%. ^{1}H NMR (400 MHz, $CDCL_3$): δ 7.74 (d, J = 15.7 Hz, 1H), 7.69 (d, J = 15.8 Hz, 1H), 7.55 (d, J = 8.9 Hz, 2H), 7.22 (dd, J = 8.3, 1.9 Hz, 1H), 7.17 (d, J = 1.9 Hz, 1H), 6.97 (d, J = 15.8 Hz, 1H), 6.92 (d, J = 15.8 Hz, 1H), 6.91 (d, J = 8.4 Hz, 1H), 6.72 (d, J = 8.9 Hz, 2H), 3.97 (s, 3H), 3.95 (s, 3H), 3.06 (s, 6H). MS (ESI): m/z calcd for $C_{21}H_{23}NO_3$, 337.17; found, 338.15 ($M + H^+$).

(1E,4E)-1-(3,5-Dimethoxyphenyl)-5-(4-(dimethylamino)phenyl)penta-1,4-dien-3-one (**36**). Compound **36** was prepared following general procedure A. Yield, 70.4%. ^{1}H NMR (400 MHz, $CDCL_3$): δ 7.72 (d, J = 15.7 Hz, 1H), 7.62 (d, J = 15.8 Hz, 1H), 7.53 (d, J = 8.9 Hz, 2H), 7.05 (d, J = 15.8 Hz, 1H), 6.89 (d, J = 15.8 Hz, 1H), 6.76 (s, 2H), 6.70 (d, J = 8.9 Hz, 2H), 6.51 (s, 1H), 3.84 (s, 6H), 3.05 (s, 6H). MS (ESI): m/z calcd for $C_{21}H_{23}NO_3$, 337.17; found, 338.15 ($M + H^+$).

(1E,4E)-1-(2,4-Dimethoxyphenyl)-5-(4-(dimethylamino)phenyl)penta-1,4-dien-3-one (**37**). Compound **37** was prepared following general procedure A. Yield, 71.4%. ^{1}H NMR (400 MHz, $CDCL_3$): δ 7.97 (d, J = 16.1 Hz, 1H), 7.69 (d, J = 15.7 Hz, 1H), 7.55 (d, J = 8.6 Hz, 1H), 7.52 (d, J = 8.9 Hz, 2H), 7.05 (d, J = 16.0 Hz, 1H), 6.92 (d, J = 15.7 Hz, 1H), 6.69 (d, J = 8.9 Hz, 2H), 6.53 (dd, J = 8.6, 2.4 Hz, 1H), 6.47 (d, J = 2.3 Hz, 1H), 3.90 (s, 3H), 3.85 (s, 3H), 3.03 (s, 6H). MS (ESI): m/z calcd for $C_{21}H_{23}NO_3$, 337.17; found, 338.10 ($M + H^+$).

(1E,4E)-1-(4-(Dimethylamino)phenyl)-5-(3,4,5-trimethoxyphenyl)penta-1,4-dien-3-one (**38**). Compound **38** was prepared following general procedure A. Yield, 71.6%. ^{1}H NMR (400 MHz, $CDCL_3$): δ 7.73 (d, J = 15.7 Hz, 1H), 7.63 (d, J = 15.8 Hz, 1H), 7.53 (d, J = 8.7 Hz, 2H), 6.97 (d, J = 15.8 Hz, 1H), 6.90 (d, J = 15.7 Hz, 1H), 6.84 (s, 2H), 6.69 (d, J = 8.7 Hz, 2H), 3.92 (s, 6H), 3.90 (s, 3H), 3.05 (s, 6H). MS (ESI): m/z calcd for $C_{22}H_{25}NO_4$, 367.18; found, 368.05 ($M + H^+$).

(1E,4E)-1-(4-(Dimethylamino)phenyl)-5-(2,4,6-trimethoxyphenyl)-penta-1,4-dien-3-one (**39**). Compound **39** was prepared following general procedure A. Yield, 58.8%. ^{1}H NMR (400 MHz, $CDCL_3$): δ 8.14 (d, J = 16.1 Hz, 1H), 7.67 (d, J = 15.7 Hz, 1H), 7.52 (d, J = 8.9 Hz, 2H), 7.41 (d, J = 16.1 Hz, 1H), 6.93 (d, J = 15.7 Hz, 1H), 6.69 (d, J = 8.9 Hz, 2H), 6.14 (s, 2H), 3.90 (s, 6H), 3.86 (s, 3H), 3.03 (s, 6H). MS (ESI): m/z calcd for $C_{22}H_{25}NO_4$, 367.18; found, 368.05 ($M + H^+$).

(1E,4E)-1-(4-(Benzyloxy)-3-methoxyphenyl)-5-(4-(dimethylamino)phenyl)penta-1,4-dien-3-one (**40**). Compound **40** was prepared following general procedure A. Yield, 61.6%. ^{1}H NMR (400 MHz, $CDCL_3$): δ 7.71 (d, J = 15.7 Hz, 1H), 7.65 (d, J = 15.8 Hz, 1H), 7.52 (d, J = 8.9 Hz, 2H), 7.45 (d, J = 8.4 Hz, 2H), 7.42−7.35 (m, 2H), 7.32 (d, J = 7.1 Hz, 1H), 7.16 (d, J = 1.9 Hz, 1H), 7.13 (dd, J = 8.3, 2.0 Hz, 1H), 6.94 (d, J = 15.8 Hz, 1H), 6.90 (d, J = 8.7 Hz, 1H), 6.89 (d, J = 15.6 Hz, 1H), 6.69 (d, J = 8.9 Hz, 2H), 5.21 (s, 2H), 3.95 (s, 3H), 3.04 (s, 6H). MS (ESI): m/z calcd for $C_{27}H_{27}NO_3$, 413.20; found, 414.20 ($M + H^+$).

(1E,4E)-1-(4-Bromo-2-hydroxyphenyl)-5-(4-(dimethylamino)phenyl)penta-1,4-dien-3-one (**41**). Compound **41** was prepared following general procedure A. Yield, 15.0%. ^{1}H NMR (400 MHz, CD_3OD): δ 7.93 (d, J = 16.0 Hz, 1H), 7.89 (s, 1H), 7.76 (d, J = 2.7 Hz, 1H), 7.74 (d, J = 16.4 Hz, 1H), 7.56 (d, J = 8.9 Hz, 2H), 7.32 (dd, J = 9.2, 3.0 Hz, 1H), 7.29 (d, J = 16.0 Hz, 1H), 6.94 (d, J = 15.7 Hz, 1H), 6.80 (d, J = 8.7 Hz, 1H), 6.75 (d, J = 9.0 Hz, 2H), 3.04 (s, 6H). MS (ESI): m/z calcd for $C_{19}H_{18}BrNO_2$, 371.05; found, 372.00 ($M + H^+$).

(1E,4E)-1-(4-(Dimethylamino)phenyl)-5-(3-phenoxyphenyl)penta-1,4-dien-3-one (**42**). Compound **42** was prepared following general procedure A. Yield, 83.9%. ^{1}H NMR (400 MHz, $CDCL_3$): δ 7.70 (d, J = 15.7 Hz, 1H), 7.64 (d, J = 15.9 Hz, 1H), 7.51 (d, J = 8.8 Hz, 2H), 7.42−7.31 (m, 4H), 7.25 (s, 1H), 7.15 (t, J = 7.4 Hz, 1H), 7.08−6.99 (m, 4H), 6.85 (d, J = 15.7 Hz, 1H), 6.69 (d, J = 8.8 Hz, 2H), 3.04 (s, 6H). MS (ESI): m/z calcd for $C_{25}H_{23}NO_2$, 369.17; found, 370.15 ($M + H^+$).

(1E,4E)-1-(2-(Benzyloxy)-4-nitrophenyl)-5-(4-(dimethylamino)phenyl)penta-1,4-dien-3-one (**43**). Compound **43** was prepared following general procedure A. Yield, 83.3%. ^{1}H NMR (400 MHz, $CDCL_3$): δ 8.54 (d, J = 2.8 Hz, 1H), 8.20 (dd, J = 9.1, 2.8 Hz, 1H), 8.02 (d, J = 16.0 Hz, 1H), 7.67 (d, J = 15.8 Hz, 1H), 7.56−7.36 (m, 7H), 7.30 (d, J = 15.9 Hz, 1H), 7.05 (d, J = 9.2 Hz, 1H), 6.82 (d, J = 15.7 Hz, 1H), 6.70 (d, J = 8.9 Hz, 2H), 5.30 (s, 2H), 3.06 (s, 6H). MS (ESI): m/z calcd for $C_{26}H_{24}N_2O_4$, 428.17; found, 429.15 ($M + H^+$).